

FINAL REPORT ~ FHWA-OK-26-01

# EFFECTIVENESS OF MAGNESIUM- ALUMINO-LIQUID PHOSPHATE-BASED CONCRETE AS A REPAIR MATERIAL

David Darwin, Ph.D., P.E.  
Matthew O'Reilly, Ph.D., P.E.  
Mohsen Salavati Khoshghalb

Department of Civil, Environmental & Architectural Engineering  
The University of Kansas  
Lawrence, Kansas

October 2025



**OKLAHOMA**  
Transportation

The Oklahoma Department of Transportation (ODOT) ensures that no person or groups of persons shall, on the grounds of race, color, sex, religion, national origin, age, disability, retaliation or genetic information, be excluded from participation in, be denied the benefits of, or be otherwise subjected to discrimination under any and all programs, services, or activities administered by ODOT, its recipients, sub-recipients, and contractors. To request an accommodation please contact the ADA Coordinator at 405-521-4140 or the Oklahoma Relay Service at 1-800-722-0353. If you have any ADA or Title VI questions email ODOT-ada-titlevi@odot.org.

The contents of this report reflect the views of the author(s) who is responsible for the facts and the accuracy of the data presented herein. The contents do not necessarily reflect the views of the Oklahoma Department of Transportation or the Federal Highway Administration. This report does not constitute a standard, specification, or regulation. While trade names may be used in this report, it is not intended as an endorsement of any machine, contractor, process, or product.

# **EFFECTIVENESS OF MAGNESIUM-ALUMINO-LIQUID PHOSPHATE-BASED CONCRETE AS A REPAIR MATERIAL**

**FINAL REPORT ~ FHWA-OK-26-01**  
ODOT SPR ITEM NUMBER 2317

**Submitted to:**  
Office of Research and Implementation  
Oklahoma Department of Transportation

**Submitted by:**  
David Darwin, Ph.D., P.E.  
Matthew O'Reilly, Ph.D., P.E.  
Mohsen Salavati Khoshghalb

Department of Civil, Environmental & Architectural Engineering  
The University of Kansas



October 2025

## TECHNICAL REPORT DOCUMENTATION PAGE

1. REPORT NO. FHWA-OK-26-01	2. GOVERNMENT ACCESSION NO.	3. RECIPIENT'S CATALOG NO.	
4. TITLE AND SUBTITLE <b>EFFECTIVENESS OF MAGNESIUM-ALUMINO-LIQUID PHOSPHATE-BASED CONCRETE AS A REPAIR MATERIAL</b>		5. REPORT DATE Oct 2025	
		6. PERFORMING ORGANIZATION CODE	
7. AUTHOR(S) David Darwin, Matthew O'Reilly, and Mohsen Salavati-Khoshghalb		8. PERFORMING ORGANIZATION REPORT SM Report No. 170	
9. PERFORMING ORGANIZATION NAME AND ADDRESS University of Kansas Center for Research, Inc. 2585 Irving Hill Road Lawrence, Kansas 66045-7563		10. WORK UNIT NO.	
		11. CONTRACT OR GRANT NO. ODOT SPR Item Number 2317	
12. SPONSORING AGENCY NAME AND ADDRESS Oklahoma Transportation Office of Research and Implementation 200 N.E. 21st Street, Rm. 3A7 Oklahoma City, OK 73105		13. TYPE OF REPORT AND PERIOD COVERED Final Report Jan 2023 - Oct 2025	
		14. SPONSORING AGENCY CODE	
15. SUPPLEMENTARY NOTES <a href="#">Click here to enter text.</a>			
16. ABSTRACT <p>A proprietary magnesium-alumino-liquid-phosphate (MALP) concrete, manufactured by Phoscrete Corporation, is a rapid-setting repair material promoted for its ability to bond with portland cement concrete and protect reinforcing steel against corrosion. A related product, magnesium-potassium-phosphate (MKP) concrete, offers slower setting for easier placement, while MKP-VO combines MKP with MALP for vertical or overhead applications. This study evaluates the durability and protective performance of MALP (with and without the organic additive Endure), MKP, and MKP-VO under aggressive conditions relevant to reinforced concrete infrastructure. The study includes more than 120 corrosion specimens, 39 freeze-thaw specimens, 24 scaling specimens, and 39 shrinkage specimens to assess: (1) corrosion protection provided to reinforcing steel in cracked and uncracked concrete, including cases with pre-corroded reinforcement; (2) resistance to freeze-thaw cycling; (3) resistance to scaling under freezing and thawing with deicing salts; and (4) shrinkage behavior. Specimens in which MALP completely enclosed the reinforcing steel exhibited excellent corrosion performance. Specimens combining MALP with conventional concrete showed very low macrocell corrosion rates, but cracked specimens exhibited high total (macrocell plus microcell) corrosion rates. Field test specimens with MALP repair regions provided poorer corrosion performance than similar specimens cast with good quality conventional concrete, suggesting that the presence of cracks at the interface of repair regions permit water, oxygen, and deicing chemicals to reach the reinforcing steel. MKP did not provide good corrosion protection. MALP showed excellent freeze-thaw durability, while MKP failed quickly and MKP-VO performed moderately well but degraded over time. In the scaling test, MALP did not perform well while MKP and MKP-VO showed excellent scaling resistance. MALP and MKP-VO shrink while MKP exhibits initial expansion followed by shrinkage at a slower rate than MALP and maintains a net expansion.</p>			
17. KEY WORDS Magnesium-alumino-liquid-phosphate (MALP) concrete, Magnesium-potassium-phosphate (MKP) concrete, reinforced concrete repair, rapid-setting concrete, corrosion protection, freeze-thaw resistance		18. DISTRIBUTION STATEMENT No restrictions. This publication is available from the Office of Research and Implementation, Oklahoma DOT.	
19. SECURITY CLASSIF. (OF THIS REPORT) Unclassified		20. SECURITY CLASSIF. (OF THIS PAGE) Unclassified	21. NO. OF PAGES 60
		22. PRICE N/A	

Form DOT F 1700.7 (08/72)

# SI\* (MODERN METRIC) CONVERSION FACTORS

## APPROXIMATE CONVERSIONS TO SI UNITS

SYMBOL	WHEN YOU KNOW	MULTIPLY BY	TO FIND	SYMBOL
<b>LENGTH</b>				
in	inches	25.4	millimeters	mm
ft	feet	0.305	meters	m
yd	yards	0.914	meters	m
mi	miles	1.61	kilometers	km
<b>AREA</b>				
in <sup>2</sup>	square inches	645.2	square millimeters	mm <sup>2</sup>
ft <sup>2</sup>	square feet	0.093	square meters	m <sup>2</sup>
yd <sup>2</sup>	square yard	0.836	square meters	m <sup>2</sup>
ac	acres	0.405	hectares	ha
mi <sup>2</sup>	square miles	2.59	square kilometers	km <sup>2</sup>
<b>VOLUME</b>				
fl oz	fluid ounces	29.57	milliliters	mL
gal	gallons	3.785	liters	L
ft <sup>3</sup>	cubic feet	0.028	cubic meters	m <sup>3</sup>
yd <sup>3</sup>	cubic yards	0.765	cubic meters	m <sup>3</sup>
NOTE: volumes greater than 1000 L shall be shown in m <sup>3</sup>				
<b>MASS</b>				
oz	ounces	28.35	grams	g
lb	pounds	0.454	kilograms	kg
T	short tons (2000 lb)	0.907	megagrams (or "metric ton")	Mg (or "t")
<b>TEMPERATURE (exact degrees)</b>				
°F	Fahrenheit	5 (F-32)/9 or (F-32)/1.8	Celsius	°C
<b>ILLUMINATION</b>				
fc	foot-candles	10.76	lux	lx
fl	foot-Lamberts	3.426	candela/m <sup>2</sup>	cd/m <sup>2</sup>
<b>FORCE and PRESSURE or STRESS</b>				
lbf	poundforce	4.45	newtons	N
lbf/in <sup>2</sup>	poundforce per square inch	6.89	kilopascals	kPa

## APPROXIMATE CONVERSIONS FROM SI UNITS

SYMBOL	WHEN YOU KNOW	MULTIPLY BY	TO FIND	SYMBOL
<b>LENGTH</b>				
mm	millimeters	0.039	inches	in
m	meters	3.28	feet	ft
m	meters	1.09	yards	yd
km	kilometers	0.621	miles	mi
<b>AREA</b>				
mm <sup>2</sup>	square millimeters	0.0016	square inches	in <sup>2</sup>
m <sup>2</sup>	square meters	10.764	square feet	ft <sup>2</sup>
m <sup>2</sup>	square meters	1.195	square yards	yd <sup>2</sup>
ha	hectares	2.47	acres	ac
km <sup>2</sup>	square kilometers	0.386	square miles	mi <sup>2</sup>
<b>VOLUME</b>				
ml	milliliters	0.034	fluid ounces	fl oz
L	liters	0.264	gallons	gal
m <sup>3</sup>	cubic meters	35.314	cubic feet	ft <sup>3</sup>
m <sup>3</sup>	cubic meters	1.307	cubic yards	yd <sup>3</sup>
<b>MASS</b>				
g	grams	0.035	ounces	oz
kg	kilograms	2.202	pounds	lb
Mg (or "t")	megagrams (or "metric ton")	1.103	short tons (2000 lb)	T
<b>TEMPERATURE (exact degrees)</b>				
°C	Celsius	1.8C+32	Fahrenheit	°F
<b>ILLUMINATION</b>				
lx	lux	0.0929	foot-candles	fc
cd/m <sup>2</sup>	candela/m <sup>2</sup>	0.2919	foot-Lamberts	fl
<b>FORCE and PRESSURE or STRESS</b>				
N	newtons	0.225	poundforce	lbf
kPa	kilopascals	0.145	poundforce per square	lbf/in <sup>2</sup>

## **ACKNOWLEDGEMENTS:**

This study was supported by the Oklahoma Department of Transportation (ODOT SP&R Item Number 2317). Material support was provided by the Phoscrete Corporation.

## TABLE OF CONTENTS

<b>CHAPTER 1: INTRODUCTION .....</b>	<b>1</b>
1.1    Objectives .....	1
1.2    Previous Work.....	2
1.3    Scope.....	3
<b>CHAPTER 2: EXPERIMENTAL WORK.....</b>	<b>4</b>
2.1    Materials .....	4
2.2    Mixture proportions .....	4
2.3    Mixing procedures .....	5
2.4    Corrosion test .....	6
2.5    Linear Polarization Resistance Measurements.....	17
2.6    Freeze-thaw tests and scaling tests .....	18
2.7    Shrinkage tests .....	20
<b>CHAPTER 3: TEST RESULTS.....</b>	<b>22</b>
3.1    Corrosion test results.....	22
3.2    Freeze-thaw and scaling test results.....	40
3.3    Shrinkage test results .....	44
<b>CHAPTER 4: ANALYSIS OF TEST RESULTS .....</b>	<b>46</b>
4.1    Corrosion resistance .....	46
4.2    Freeze-thaw test.....	47
4.3    Scaling test.....	48
4.4    Shrinkage test.....	48
<b>CHAPTER 5: SUMMARY AND CONCLUSIONS .....</b>	<b>50</b>
5.1    Summary .....	50
5.2    Conclusions .....	50
5.3    Recommendations .....	51
<b>CHAPTER 6: REFERENCES .....</b>	<b>52</b>

## LIST OF FIGURES

<b>Figure 2.1:</b> 5-Gallon Bucket and Drill-Mounted Mixer .....	6
<b>Figure 2.2:</b> Test specimens for (a) Beam Test and (b) Cracked Beam Test .....	8
<b>Figure 2.3:</b> Field Test Specimens for Phoscrete/Conv.....	12
<b>Figure 2.4:</b> Field Test Specimens for Monolithic Conventional concrete.....	12
<b>Figure 2.5:</b> Top and side Field Test Specimens for Monolithic-Phoscrete . <b>Error! Bookmark not defined.</b>	
<b>Figure 2.6:</b> MALP/Conv field test specimen with the edges of the repair patch aligned directly above the reinforcement (specimens with "A" in title) before casting .....	14
<b>Figure 2.7:</b> MALP/Conv field test specimen with the edges of the repair patch aligned between reinforcing bars (specimens with "B" in title) before casting.....	14
<b>Figure 2.8:</b> Field test specimen containing conventional concrete without MALP .....	15
<b>Figure 2.9:</b> Field test specimen containing conventional concrete without MALP and with simulated cracks.....	15
<b>Figure 2.10:</b> Field test specimen containing MALP.....	16
<b>Figure 2.11:</b> Freeze-thaw specimen, a) monolithic, b) vertical interface, c) horizontal interface	19
<b>Figure 3.1:</b> Average macrocell corrosion rates of specimens in the beam test .....	24
<b>Figure 3.2:</b> Average top mat corrosion potentials vs. CSE of specimens containing MALP and MKP in the beam test.....	25
<b>Figure 3.3:</b> Average macrocell corrosion rates of specimens in the cracked-beam test.....	27
<b>Figure 3.4:</b> Average top mat corrosion potentials vs. CSE of specimens in the cracked-beam test.....	28
<b>Figure 3.5:</b> Cracked beam specimens with and without Endure at the end of 96 weeks.....	31
<b>Figure 3.6:</b> Top mat steel bars from MALP cracked beam specimens with and without Endure at the end of 96 weeks .....	32
<b>Figure 3.7:</b> MALP beam specimens with and without Endure at the end of 96 weeks .....	32
<b>Figure 3.8:</b> Top mat steel bars from MALP beam specimens with and without Endure at the end of 96 weeks.....	33
<b>Figure 3.9:</b> MKP and MKP-VO beam specimens at the end of 96 weeks .....	33
<b>Figure 3.10:</b> Top mat steel bars from MKP and MKP-VO beam specimens at the end of 96 weeks .....	34
<b>Figure 3.11:</b> MKP and MKP-VO cracked beam specimens at the end of 96 weeks .....	34
<b>Figure 3.12:</b> Top mat steel bars from MKP and MKP-VO cracked beam specimens at the end of 96 weeks.....	35
<b>Figure 3.13(a):</b> Average macrocell corrosion rates of field test specimens .....	37
<b>Figure 3.13(b):</b> Average macrocell corrosion rates of field test specimens incorporating MALP .....	38
<b>Figure 3.14(a):</b> Average top mat corrosion potentials vs. CSE of field test specimens .....	39
<b>Figure 3.14(b):</b> Average top mat corrosion potentials vs. CSE of field test specimens incorporating MALP .....	40
<b>Figure 3.15:</b> Percentage of initial dynamic modulus of elasticity vs. number of freeze-thaw cycles.....	41
<b>Figure 3.16:</b> Percentage of initial dynamic modulus of elasticity vs. number of freeze-thaw cycles.....	42
<b>Figure 3.17:</b> Three MKP specimens after 864 cycles in Freeze-thaw machine.....	43
<b>Figure 3.18:</b> Average mass loss per ft <sup>2</sup> vs. number of cycles in the scaling test .....	44

**Figure 3.19:** Average shrinkage, microstrain vs. number of days after casting for specimens containing MALP, MKP and MKP-VO ..... 45

## LIST OF TABLES

<b>Table 2.1:</b> Mixture proportions of conventional concrete for lab and field specimens based on SSD aggregate .....	5
<b>Table 2.2:</b> Mixture proportions of Low-quality conventional concrete (w/c = 0.6) for lab and field specimens based on SSD aggregate .....	5
<b>Table 2.3:</b> Corrosion resistance test program .....	17
<b>Table 2.4:</b> Freeze-thaw test program .....	19
<b>Table 2.5:</b> Scaling test program .....	20
<b>Table 2.6:</b> Free shrinkage test program .....	21
<b>Table 3.1:</b> Average Macrocell and Total Corrosion Rates at Week 72 .....	29
<b>Table 3.2:</b> Average Macrocell and Total Corrosion Rates at Week 60 .....	30
<b>Table 3.3:</b> Crack width in field test specimens with repair patch .....	45



# CHAPTER 1: INTRODUCTION

Phoscrete, a proprietary magnesium-alumino-liquid-phosphate (MALP) concrete, is a repair material that is formed by an exothermic reaction between a prepackaged dry component, consisting of magnesium oxide, calcined aluminosilicates, graded aggregates, and fibers, and a liquid phosphate activator. Claims for Phoscrete MALP concrete include statements that it can bind to clean, sound portland cement concrete and provide a level of corrosion protection to reinforcing steel. The material sets rapidly and gains strength in less than an hour. It has been used as a rapid repair material for reinforced concrete transportation structures, requiring minimal labor, although its rapid set can make it difficult to work with. It is claimed to be slightly expansive during early curing (Floyd et al. 2021), which should reduce crack widths between the repair and adjacent concrete shortly after casting, and it has a lower pH than newly cast portland cement concrete, which should reduce the potential for corrosion of reinforcing steel that is continuous between the repair and older surrounding concrete that has a lower pH due to carbonation (often referred to as the “halo” or “ring-anode” effect). The Phoscrete Corporation has also developed a magnesium-potassium-phosphate (MKP) cement-based concrete repair material consisting of magnesium oxide, potassium phosphate, calcined aluminosilicates, graded aggregates and fibers that uses water rather than a liquid activator. It sets more slowly than MALP, giving more working time, behavior that is particularly important in hot weather.

This study involves the evaluation of MALP containing Endure, an organic admixture designed to improve the resistance of MALP to freeze-thaw damage and salt scaling, MALP without Endure, MKP, and MKP-VO, which contains MKP, Endure, and some MALP and is formulated for vertical or overhead placement.

The materials are evaluated based on their ability to (1) protect reinforcing steel against corrosion where uncracked and cracked concrete is subject to chlorides, as stand-alone materials and in conjunction with conventional concrete, (2) withstand cycles of freezing and thawing as stand-alone materials and in conjunction with conventional concrete, and (3) withstand exposure to conditions causing scaling under freezing and thawing, and (4) exhibit minimum shrinkage so as to limit crack width at the edge of repairs.

## 1.1 Objectives

The objectives of this study are to determine the extent to which MALP, with and without Endure, and the MKP products:

1. Provide corrosion protection to reinforcing bars that are either in a passive state or undergoing active corrosion, in both uncracked and cracked concrete.
2. Mitigate the corrosion of reinforcing steel that remains continuous between newly repaired areas and older surrounding concrete over time.
3. Withstand freeze-thaw cycles, both independently and in combination with portland cement concrete.
4. Minimize crack widths at the repair boundary as a function of time.

## 1.2 Previous Work

Prior to this research, most of the information available on the materials in this study was based on literature provided by the producing company, Phoscrete Corporation. Four products are under study: (1) Magnesium-alumino-liquid-phosphate (MALP) concrete, a proprietary product, produced under the trade name Phoscrete, is formed by an exothermic reaction between a prepackaged dry component—consisting of magnesium, calcined aluminosilicates, graded aggregates, and fibers—a liquid phosphate activator and Endure. (2) Magnesium-Alumino-Liquid Phosphate-Based Concrete without Endure. (3) a magnesium-potassium-phosphate (MKP) cement-based concrete repair material, also developed by The Phoscrete Corporation, consisting of magnesium oxide, potassium phosphate, calcined aluminosilicates, graded aggregates and fibers that uses water rather than a liquid activator, and (4) a version of MKP, MKP-VO, designed for vertical or overhead placement. The latter material was added to the study at the request of ODOT after the project was initiated.

One area with little available information was the ability of MALP to limit the corrosion of reinforcing steel in concrete. Phoscrete Corporation (2021) claimed that because the material has a lower pH than portland cement concrete, MALP is less likely to cause the “Ring Anode” effect – that is, accelerating corrosion in reinforcing steel adjacent to repaired areas. The effect can occur when a portland cement-based concrete repair is used because the material surrounding the repair typically has a lower pH than new portland cement concrete due to carbonation, setting up a difference in the corrosion potential between the two concretes that tends to increase the probability of corrosion in the older, lower pH material due to galvanic corrosion. Using MALP also sets up a difference in potential between it and the material surrounding the repair, but the lower pH of MALP would result in the surrounding material being less active (and therefore less prone to corrosion), while the low permeability of the MALP repair prevents moisture and oxygen from reaching the reinforcement in the repair region, thus preventing corrosion from occurring.

The Phoscrete Corporation has not published data on the corrosion performance of MALP. The only published information on the effect of MALP on the corrosion performance of reinforcing steel is that described by Floyd et al. (2021). In their study, Floyd et al. performed “small-scale” corrosion tests with each specimen consisting of half conventional concrete and half repair material for each of three repair materials. In a number of specimens, the conventional concrete contained admixed sodium chloride in quantities equal to 4 and 8% by weight of cement to represent concrete that has been in service and exposed to differing levels of chloride. Three No. 3 bars were cast in both the conventional concrete and the repair material and connected across a 100-ohm resistor. After curing, the specimens were placed in a 5% sodium chloride solution and the macrocell current, used as a measure of macrocell corrosion loss, based on the voltage drop across the resistor was monitored for 10 weeks, after which the reinforcing steel in the specimens with 4 and 8% admixed sodium chloride was exposed for visual inspection. Macrocell corrosion is a type of corrosion that occurs when an actively corroding (anodic) steel bar is electrically coupled through the concrete electrolyte to a passive bar or one corroding at a lower rate. This separation of anode and cathode often results from differences in composition, bar size, or surrounding environment such as rebar spanning old and repair concrete. This contrasts with microcell corrosion, which happens locally on a single steel bar where small adjacent areas act as anode and cathode due to surface irregularities. Microcell corrosion occurs naturally to some extent on all reinforcing steel, without requiring

separated bars or different environments. Total corrosion loss is the sum of macrocell and microcell corrosion.

Floyd et al. (2021) also performed large-scale corrosion tests. In this case, the specimens consisted of sections taken from bridge decks from which concrete was removed, exposing No. 5 reinforcing bars, and replacing the concrete with one of the repair materials being evaluated in the study. The bars were then subjected to a 0.2 A direct current, forcing the bars to corrode, for 70 days. The specimens containing MALP seemed to secrete a green liquid, possibly an iron (II) phosphate compound resulting from a reaction between the oxidized iron and MALP. The test specimens were autopsied, which revealed that the steel in the MALP specimen had undergone pitting corrosion in the specimens with 8% admixed chlorides by weight of cement.

The two tests employed by Floyd et al. (2021) have a number of drawbacks, and neither is widely used to evaluate the corrosion performance of reinforcing steel in concrete. For the small-scale tests, admixed chlorides will not be as detrimental to the corrosion of reinforcing steel as the same quantity of chlorides penetrating into concrete, because admixed chlorides tend to be bound in the hydration products, whereas chlorides that penetrate into concrete remain in the concrete pores and are fully available to accelerate corrosion. The use of a 100-ohm resistor, rather than the more widely used 10-ohm resistor, limits macrocell corrosion, and the test procedure is not designed to measure microcell as well as macrocell corrosion, which can be substantial. The large-scale test provides no information about the ability of the surrounding concrete to limit corrosion, with the exception that the corrosion loss forced by the impressed current will be sensitive to the ionic mobility within the concrete. The large-scale tests showed that the repair materials gave similar results, although the specimens with MALP concrete exhibited a lower voltage for the 0.2 A current than the other specimens, indicating greater ion mobility and potentially greater corrosion in the field. The test, however, would be expected to result in the same corrosion loss in all specimens because the impressed current was the same. The test does not provide a measure of the expected corrosion behavior of a system in the field. As a result, the ability of MALP concrete to limit corrosion of reinforcing steel remains an open question.

Studies of non-proprietary MALP include mixtures used for airfield pavements (Ramsey et al. 2020), flexural properties and microstructure of MALP made with natural fiber (Zhang et al. 2020), and applications in ultra-high-performance concrete (Qin et al. 2022).

### 1.3 Scope

This study aims to achieve the objectives outlined in Section 1.1 by evaluating the performance of MALP and MKP cements through four distinct experimental tests, as described in Chapter 2. To accomplish this, more than 120 corrosion specimens, 39 freeze–thaw specimens, 24 scaling specimens, and 39 shrinkage specimens were prepared and examined. These tests collectively address the durability and corrosion performance of the MALP materials under different environmental and structural conditions. This study examines the performance of MALP and MKP cements in mitigating reinforcement corrosion, withstanding freeze–thaw exposure, resisting surface scaling, and minimizing shrinkage-induced cracking. The results provide useful insight into how these materials can be applied as repair products to protect reinforcing steel.

## CHAPTER 2: EXPERIMENTAL WORK

The research discussed in this report is focused on (1) evaluating the corrosion performance of uncorroded and corroded reinforcing steel in cracked and uncracked concrete, (2) evaluating the freeze-thaw performance of the materials individually and in conjunction with conventional concrete, (3) evaluating the scaling performance of the materials individually, and (4) evaluating the shrinkage properties of the materials to minimize crack widths adjacent to sound concrete at a repair site. The specimens and test methods used to evaluate these materials are described below.

### 2.1 Materials

Four materials are under study:

Magnesium-Alumino-Liquid Phosphate-Based Concrete with Endure (MALP-E): Sold under the trade name Phoscrete, MALP is formed through an exothermic reaction that occurs when a prepackaged dry mixture, comprised of magnesium, calcined aluminosilicates, graded aggregates, and fibers, is combined with a liquid phosphate activator. Endure is an organic admixture designed to improve the resistance of Phoscrete MALP to freeze-thaw damage and salt scaling.

Magnesium-Alumino-Liquid Phosphate-Based Concrete without Endure (MALP-NE).

Magnesium-Potassium-Phosphate-Based Concrete (MKP): MKP cement is formed due to a reaction between potassium dihydrogen phosphate and magnesia in the presence of water. The material exhibits rapid setting, although more slowly than MALP, and achieves significant early strength. The dry mix is composed of magnesium oxide, potassium phosphate, aluminosilicates, aggregates, and reinforcing fibers, which are mixed with water (13% of the weight of dry materials) and Endure.

Magnesium-Potassium-Phosphate-Based Concrete for Vertical/Overhead Placement (MKP-VO): A modified version of MKP that is used for vertical or overhead placement. MKP-VO exhibits accelerated setting and hardening characteristics. MKP-VO contains finer aggregates than MKP, making it less permeable. A pre-measured VO-Admix jar containing 4 fluid ounces of Endure and 4 fluid ounces of MALP activator is used for mixing along with water (13.3% of the weight of dry materials).

Conventional air-entrained concrete is also evaluated both as a control and for specimens containing both MALP and conventional concrete.

### 2.2 Mixture proportions

MALP-E is prepared by mixing a 55 lb bag of dry material, a premeasured plastic jar (107 oz) of activator, and 10 oz of Endure. MALP-E is prepared by mixing a 55 lb bag of dry material with a premeasured plastic jar of activator. MKP is prepared by mixing a 55 lb bag of dry material, 7.15 lb of water, and 10 oz of Endure, and MKP-VO is prepared by mixing a 22 lb bag of material with 2.93 lb of water, 8 oz of Endure, and 4 oz of the phosphate activator used with MALP. One bag of MALP or MKP has a yield of approximately 0.4 ft<sup>3</sup>, whereas one bag of MKP-VO has a yield of approximately 0.2 ft<sup>3</sup>.

Members were also cast with conventional concrete and a representation of low-quality concrete. The mixture proportions for the conventional concrete are shown in Table 2.1. The conventional concrete had a water/cement ratio (*w/c*) of 0.45 and a nominal air content of 6%. The mixture proportions for the low-quality concrete (*w/c* = 0.6) are shown in Table 2.2. Low-quality concrete was intentionally used in experiments to accelerate corrosion and highlight performance differences in materials under different conditions. For the field test specimens, due to the large volume of concrete required and the need to cast the specimens quickly using the same material, the concrete was ordered from Midwest Concrete Materials Company.

**Table 2.1:** Mixture proportions of conventional concrete for lab and field specimens based on SSD aggregate.

Cement lb/yd <sup>3</sup>	Water lb/yd <sup>3</sup>	Coarse Aggregate lb/yd <sup>3</sup>	Fine Aggregate lb/yd <sup>3</sup>	Air Entraining Agent oz/yd <sup>3</sup>
598	270	1473	1436	68.8

**Table 2.2:** Mixture proportions of low-quality conventional concrete (*w/c* = 0.6) for lab and field specimens based on SSD aggregate.

Cement lb/yd <sup>3</sup>	Water lb/yd <sup>3</sup>	Coarse Aggregate lb/yd <sup>3</sup>	Fine Aggregate lb/yd <sup>3</sup>	Air Entraining Agent oz/yd <sup>3</sup>
450	270	1473	1559	160

The materials used in the conventional and low-quality concrete mixtures were:

Cement -Type IL Ash Grove.

Water – Municipal tap water from the city of Lawrence.

Coarse aggregate – crushed limestone from Midwest Concrete Materials. Nominal maximum size 0.75 in. (19 mm), bulk specific gravity (SSD) = 2.63, absorption 2.64 %, unit weight = 96.12 lb/ft<sup>3</sup> (1540 kg/m<sup>3</sup>).

Fine aggregate – Kansas River sand – Midwest Concrete Materials. Bulk specific gravity (SSD) = 2.62, absorption (dry) = 0.64 %, fineness modulus = 2.72.

Air-Entraining Agent- Daravair 1400

### 2.3 Mixing procedures

Following the manufacturer's recommendations, MALP-E, MALP-NE, MKP, and MKP-VO were mixed in a 5-gallon plastic bucket using a drill-mounted augur mixer for one minute, as shown in Figure 2.1. For MALP-E, the activator was added first, followed by Endure and, finally, the dry material. A comparable procedure was employed for MALP-NE, without Endure. For MKP, water is added to the bucket first, followed by Endure, and the dry material. A similar procedure is followed for MKP-VO.

A counter-current pan mixer was used for mixing conventional and low-quality concrete in the lab. Prior to mixing, the pan and blades were dampened. The mixer was first filled with the

coarse aggregate and 90% of the mixing water before rotation began. These materials were mixed for 1½ minutes. Portland cement was then added, and the mixture was mixed for another 1½ minutes, followed by the addition of fine aggregates and another 2 minutes of mixing. The air-entraining admixture was then added with the remaining 10% of the mixing water, followed by 4 minutes of mixing. The batch weights of the aggregates and water were adjusted for the moisture content of the aggregates.



**Figure 2.1:** Mixing material in a 5-gallon bucket and drill-mounted mixer

## 2.4 Corrosion tests

The corrosion resistance of reinforcing steel in MALP, MKP, and MKP-VO was compared to that of conventional concrete to evaluate their effectiveness as repair materials for reinforced concrete structures. Comparisons were conducted for both clean reinforcement and reinforcement that had previously been exposed to chlorides. The materials were evaluated alone and in conjunction with conventional concrete. Both Bench-Scale and Field Test Specimens were used to evaluate performance; these specimens are described below.

*Bench-Scale Tests.* Bench-scale tests, such as the Southern Exposure, ASTM G109, beam, and cracked beam tests, have been used most often to evaluate the corrosion

performance of reinforcing steel. Although these tests typically require one to two years for completion, they qualify as accelerated tests, considering that the service life of actual structures should be 30+ times as long. In this study, a modified version of the Southern Exposure specimen, the beam specimen, and the cracked beam specimen were used.

The *beam* specimen consists of a small slab with two mats of reinforcing steel (Fig. 2.2a). The top mat consists of one No. 5 bar; the bottom mat consists of two No. 5 bars. The reinforcing steel satisfied the requirements of ASTM A615. The mats are electrically connected across a 10-ohm resistor, a dam is cast around the edge of the top surface, and the sides of the concrete are sealed with epoxy. A 15% sodium chloride solution is placed inside the dam, allowing the chlorides to penetrate into the concrete. The slabs are subjected to a seven-day alternate ponding and drying regime, with ponding at 72°F (22°C) for four days and drying at 100°F (38°C) for three days. The ponding and drying regime is continued for 12 weeks. The specimens are then subjected to continuous ponding for 12 weeks, at which time the alternating ponding and drying regime begins again. The two regimes are continued for 96 weeks. Corrosion current and the corresponding corrosion rate are determined by measuring the voltage drop across the resistor. The corrosion potential of the top and bottom mats and mat-to-mat resistance are also measured. Steel with a corrosion potential more negative than  $-0.35$  V is considered to have greater than a 90 % probability that corrosion is occurring (ASTM C876). The test provides a very severe corrosion environment that, based on chloride concentrations obtained at a depth of 1 in. (25 mm) in the beam test and at a depth of 3 in. (75 mm) on bridge decks (Lindquist et al. 2006), simulates 10 years of exposure for bridge decks within the first 30 weeks and 30 years within the 96-week duration of the test.

The *cracked beam* (CB) specimen (Fig. 2.2b) is used to model the corrosion of reinforcing steel in concrete where cracks form directly above the reinforcement, as occurs in bridge decks, exposing the steel to deicing chemicals. The specimen has the same dimensions as the beam specimen. A crack is simulated parallel to and above the top reinforcing bar with the insertion of a 0.012 in. (0.3 mm) stainless steel shim when the specimen is fabricated. The shim is removed 12-24 hours after casting, leaving a direct path for chlorides to the reinforcing steel and simulating the effects of a settlement crack over the bar. A dam is cast around the specimen in a manner similar to that used for the beam specimens.

Like the beam specimen, the cracked beam specimen is subjected to cycles of wetting and drying with a 15% sodium chloride solution, continuing for 96 weeks. With conventional uncoated reinforcement, beam specimens typically exhibit corrosion initiation after 8 to 16 weeks of testing and CB specimens typically initiate corrosion during the first week of testing.

To determine the potential for galvanic corrosion, a modified version of the specimens was used. Here, the bottom half of the specimen consists of conventional concrete and the top half consists of MALP. The dimensions of the specimens are otherwise the same as shown in Figs. 2a and 2b. Several specimens were cast with pre-corroded bars to evaluate the ability of MALP to repair structures in which the steel has already been subjected to chlorides.

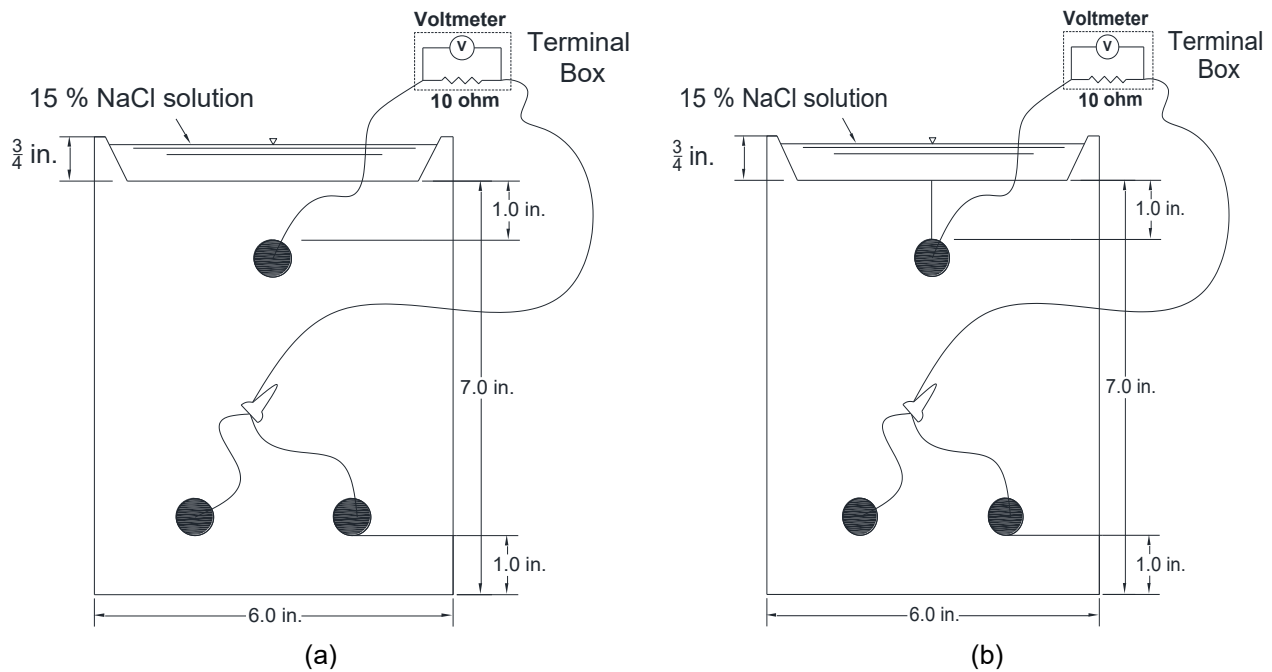


**Figure 2.2:** Test specimens for (a) Beam Test and (b) Cracked Beam Test

For the beam and cracked beam specimens, corrosion rate and corrosion potential measurements were taken weekly for 96 weeks. The area of the anode (top) bar is used to calculate the corrosion rate, which is calculated based on the voltage drop measured across the 10-ohm resistor using Faraday's equation.

$$\text{Rate} = K \frac{V m}{n F D R A} \quad (2.1)$$

where the rate is given in  $\mu\text{m}/\text{yr}$ ,

$K$  = conversion factor =  $31.5 \cdot 10^4$  amp $\cdot$  $\mu\text{m} \cdot \text{sec}/\mu\text{A} \cdot \text{cm} \cdot \text{yr}$

$V$  = measured voltage drop across resistor, millivolts

$m$  = atomic weight of the metal (for iron,  $m = 55.8 \text{ g/mol}$ ; for zinc,  $m = 65.4 \text{ g/mol}$ )

$n$  = number of ion equivalents exchanged (for iron and zinc,  $n = 2$  equivalents)

$F$  = Faraday's constant = 96485 coulombs/equivalent

$D$  = density of the metal,  $\text{g}/\text{cm}^3$  (for iron,  $D = 7.87 \text{ g}/\text{cm}^3$ ; for zinc,  $D = 7.14 \text{ g}/\text{cm}^3$ )

$R$  = resistance of resistor, ohms = 10 ohms for the test

$A$  = surface area of anode exposed to solution

In some cases, the corrosion rate may appear to be negative. This negative corrosion rate does not indicate negative corrosion; it is rather caused by minor differences in the

oxidation rate between the single anode bar and the cathode bars.

Determining the corrosion rate by taking voltage readings across the 10-ohm resistor (the macrocell corrosion rate) has the potential to miss localized corrosion, where the current flow between the anodic and cathodic reactions does not pass through the resistor placed between test bars. To capture both localized and general corrosion (referred to as the total corrosion rate) linear polarization resistance (LPR) tests (described in Section 2.4) are performed every 4 weeks. In addition, the corrosion potential is measured at both the anode and cathode using a silver-silver chloride electrode. Potential readings are converted to an equivalent copper-copper sulfate electrode (CSE) for presentation.

#### Fabrication:

Specimen fabrication for beam and cracked beam specimens is as follows:

1. Reinforcing bars were cut to 12 in. lengths using a band saw.
2. Both ends of each bar were drilled and tapped to a depth of 3/8 in. with 10-24 threading.
3. For specimens containing corroded bars, the bars were soaked in a 15% NaCl solution for three weeks prior to casting.
4. The forms were assembled, and the reinforcement was attached. Forms and reinforcement were held in place using 10-24 threaded stainless-steel machine screws.
5. Specimens were cast in an inverted position. The free surface of the concrete (the bottom of the specimen, as they were cast upside down) was finished with a trowel.
6. Specimens containing half MALP and half conventional concrete were cast in two layers, the conventional concrete (bottom side) was cast first, followed by the MALP (upper side).
7. Specimens made with conventional concrete were cured for 24 hours at room temperature under a plastic cover to minimize evaporation. Stainless-steel shims were removed from the cracked beam specimens after 12–24 hours, once the concrete had set.
8. For specimens made with conventional concrete, formwork was removed after 24 hours. Specimens were then cured for an additional two days in a plastic bag containing deionized water, followed by 25 days of air curing.
9. For specimens containing MALP, MKP, and MKP-VO, the formwork was removed immediately after setting, and the specimens were cured for 72 hours in an environmentally controlled room at a relative humidity of  $50 \pm 4\%$  and a temperature of  $73 \pm 3$  °F.
10. Prior to test initiation, wire leads were connected to the test bars using 10-24  $\times$  3/8-in. stainless-steel screws. An epoxy coating was applied to the vertical sides of the specimens and the top surface of the dams, while the top and bottom faces of the specimens were left uncoated.
11. The two mats of steel were connected to the terminal box. The specimens were kept connected across a 10-ohm resistor, except during measurements. Each specimen was placed on 2  $\times$  2 in. studs to allow air circulation underneath.

**Field Tests:** Field Test Specimens (FTS) are designed to evaluate the performance of corrosion protection systems when subjected to seasonal weather and environmental changes (Darwin et al. 2011). MALP products were evaluated both as an  $18 \times 18 \times 3$  in. patch in conventional concrete, as shown in Fig 2.3, and as Monolithic-MALP specimens, as shown in Fig. 2.4. Conventional concrete field test specimens were used as controls (Fig. 2.5).

The specimens with a MALP patch and the conventional concrete specimens have two mats of No. 5 ASTM A615 reinforcing bars, with each mat consisting of two layers of seven 42-in. long bars spaced 6 in. on center for MALP/Conv specimens. The bars in the upper layer of each mat run perpendicular to those in the lower layer. Plastic chairs are used to provide 1-in. clear cover to both the top and bottom mats of steel. Two versions of the MALP/Conv specimens were tested: one with the edges of the patch located so that the boundary of the two concretes is adjacent to bars parallel to the patch (specimens with "A" in title) (Fig. 2.3a) and one with edges of the patch perpendicular to bars in the upper layer (specimens with "B" in title) (Fig. 2.3b). Weather stripping is used on the top surface to allow for ponding of a 10% salt solution. Four bars from the top mat are electrically connected across a 10-ohm resistor to the equivalent bar in the bottom mat. Field test specimens containing conventional concrete without MALP, one with simulated cracks and one without cracks, are shown in Fig. 2.5a and 2.5b with and without cracks, respectively. Simulated cracks were placed in the specimens using a wooden frame with four slots to hold the stainless steel shims vertically.

The field test specimens consisting of just MALP measure  $18 \times 18 \times 6.5$  in. ( $0.457 \times 0.457 \times 0.17$  m), as shown in Figure 2.4. These specimens have two mats of No. 5 reinforcing bars, with each mat consisting of two layers of three 16-in. long bars spaced 6 in. on center. Four of these specimens were cast—two with cracks (one with pre-corroded reinforcement and one with reinforcement not subjected to corrosion prior to casting) and two without cracks—one with corroded reinforcement and with reinforcement not subjected to corrosion prior to casting.

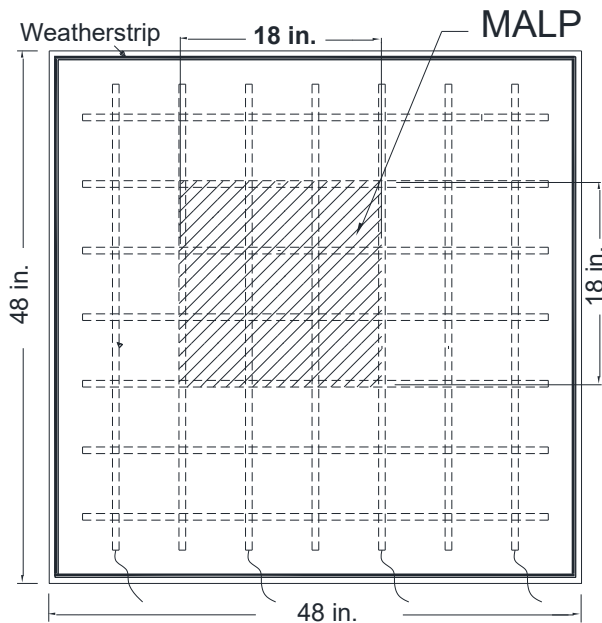
#### Fabrication:

Specimen fabrication for field test specimens is as follows:

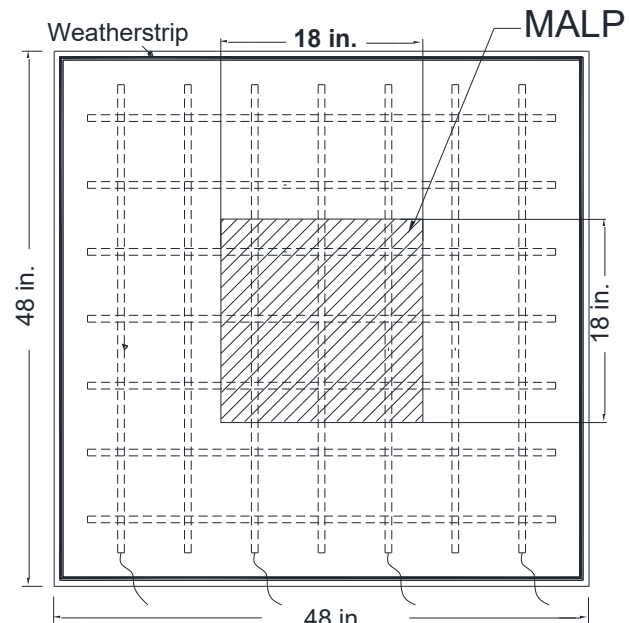
1. Reinforcing bars were cut to 42 in. lengths using a band saw.
2. One end of each bar was drilled and tapped to a depth of 3/8 in. with 10-24 threading.
3. For specimens containing corroded bars, the bars were soaked in a 15% NaCl solution for three weeks prior to casting.
4. A 36-in.-long, 16-gauge insulated multi-strand copper wire was attached to the tapped end of each test bar using a 13-mm (0.5-in.) 10-24 stainless-steel machine screw. All specimens contained four test bars, numbered 1, 3, 5, and 7, as shown in Figure 2.3.
5. The electrical connections were coated with rebar patch epoxy and fitted with heat-shrink tubing to secure the wire in place after shrinking.
6. The reinforcement was placed into the assembled formwork and supported with plastic chairs. The mats were held in position horizontally using tie wires. For specimens requiring cracks, stainless-steel shims were positioned on top of the reinforcement using a wooden frame with four slots.

7. Specimens were cast with ready-mix concrete using the mixture proportions shown in Tables 2.1 and 2.2. Consolidation was achieved with internal vibration.
8. Shims were removed from cracked specimens after 12 hours.
9. Specimens were covered with wet burlap and plastic sheeting and cured for seven days.
10. After curing, specimens were demolded and air-cured for an additional three weeks.
11. MALP with and without Endure was cast for the repair patch specimens before they were moved outdoors.
12. Seven days prior to testing, specimens were transferred to the outdoor test site at the University of Kansas West Campus. They were placed on concrete blocks to maintain a clearance of approximately 8 in. above the ground.
13. The 1-in.-wide, 0.5-in.-thick weather stripping was applied around the top edge of all specimens to allow for ponding with salt solution.

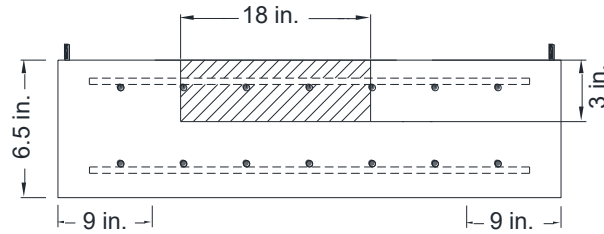
The corroded reinforcement for the bench scale and field test specimens was prepared by immersing the reinforcement in a 15% NaCl solution for three weeks.



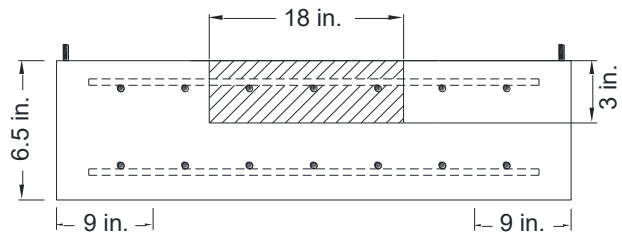
(a) Top slab-MALP/Conv



(b) Top slab-MALP/Conv

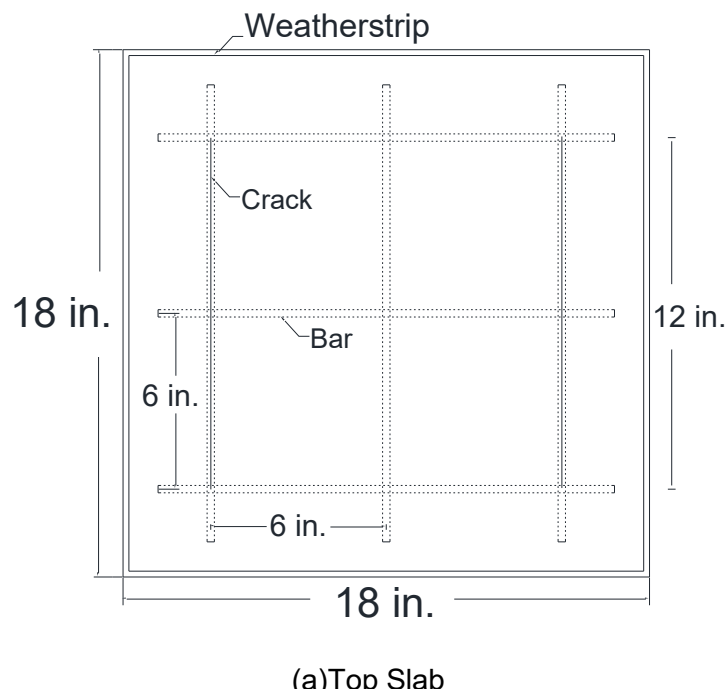


(c) Side view



(d) Side view

**Figure 2.3:** Field Test Specimens for MALP/Conv (a and c: MALP-E-A-Conv; b and d: MALP-E-B-Conv)



(a) Top Slab



(b) Side view

**Figure 2.4:** Top (a) and Side (b) View of Field Test Specimens for Monolithic-MALP Field Test Specimen

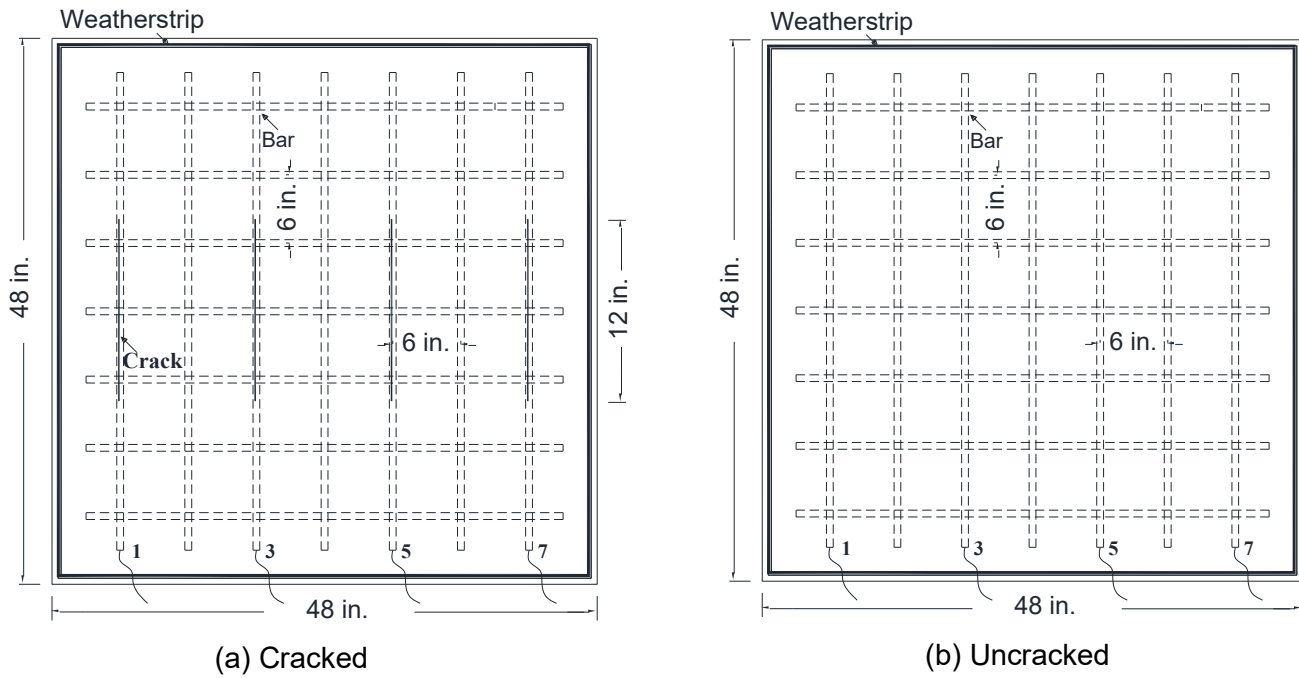


**Figure 2.5: Field Test Specimens for Monolithic Conventional Concrete**

Field test specimens are left outdoors to provide exposure to the range of weather conditions seen in the Midwest. In addition to exposure to the weather, the specimens are ponded with 10% salt solution every four weeks. For the larger (48 in.  $\times$  48 in.) specimens, this results in a salt application of 0.66 lb of salt every four weeks for a total annual salt application of 7.92 lb. For the smaller (18 in.  $\times$  18 in.) specimens, this results in a salt application of 0.092 lb every four weeks, totaling 1.1 lb annually. The application rate for the slabs is based on work by Guo et al. (2006) who found that a typical bridge deck in northeast Kansas receives an average annual salt application of 0.54 lb/ft<sup>2</sup>. In past tests, field test specimens have been evaluated for a period of five years (Darwin et al. 2011, O'Reilly et al. 2021). For this study, however, testing was limited to the time available for the study.

Figures 2.6 through 2.10 show the FTS specimen forms with the reinforcing steel and, where used, foam block-outs for regions in which MALP is used to simulate a repair prior to casting. To place the foam block-out 18 in.  $\times$  18 in.  $\times$  3 in. cardboard boxes were prepared and covered with plastic sheets to prevent water absorption from the concrete. Each cardboard box was then placed between the reinforcement, as shown in Figures 2.6 and 2.7. The reinforcement inside the box was covered with tape to protect it from contact with the foam material. The foam block-out was poured into the box one day before casting to allow it to set properly.



**Figure 2.6:** Form and reinforcing steel for MALP/Conv field test specimen showing the foam block-out used so that the edges of the repair patch aligned directly above the reinforcement (specimens with "A" in title) before casting



**Figure 2.7:** Form and reinforcing steel for MALP/Conv field test specimen showing the foam block-out used so that the edges of the repair patch aligned between reinforcing bars (specimens with "B" in title) before casting

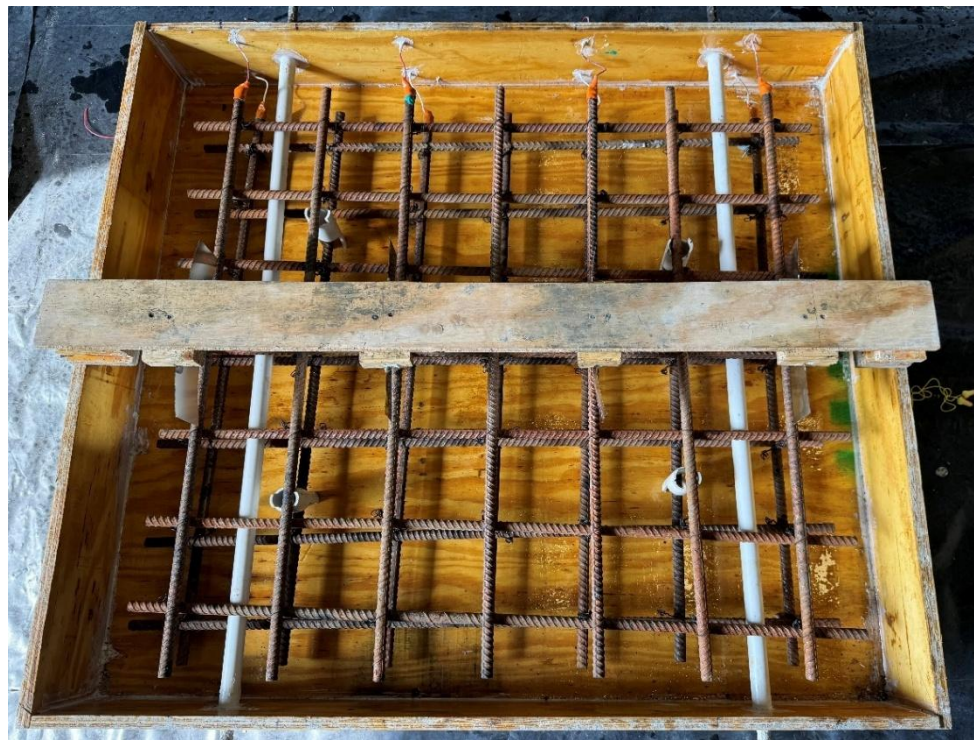


**Figure 2.8:** Form and reinforcing steel for field test specimen containing conventional concrete without MALP and with simulated cracks before casting



**Figure 2.9:** Form and reinforcing steel for field test specimen containing conventional concrete without MALP and without simulated cracks before casting



**Figure 2.10:** Form and reinforcing steel for field test specimen containing MALP before casting

*Corrosion Test Program:* The corrosion test program is summarized in Table 2.2. Most specimens were evaluated using conventional concrete ( $w/c = 0.45$ ) and Phoscrete products. Some were cast with low quality concrete ( $w/c = 0.60$ ). The majority of specimens are constructed using uncorroded steel; however, some bars are subject to corrosion prior to specimen fabrication by immersion in salt water. The MALP specimens are tested both with and without Endure.

In Table 2.3, conventional concrete is represented by the abbreviation "Conv." The designation MALP-E refers to specimens containing Magnesium–Aluminum–Liquid–Phosphate (MALP) concrete with Endure, whereas MALP-NE refers to specimens containing MALP without Endure. The term MKP is used for Magnesium–Potassium–Phosphate-based specimens, and MKP-VO denotes Magnesium–Potassium–Phosphate-based concrete designed for vertical or overhead applications. The label MALP-E/Conv. represents specimens composed of half conventional concrete and half MALP with Endure, while MALP-NE/Conv. refers to the two field test specimens that included conventional concrete and MALP without Endure as the repair patch.

**Table 2.3:** Corrosion resistance test program

	Specimen Type		
	Beam	Cracked beam	FTS
Conventional Concrete, Uncorroded Steel	-		
Conv	6	6	2*
MALP-E	5	6	2
MALP-NE	6	6	-
MKP	6	6	-
MKP-VO	3	3	-
MALP-E/Conv	3	3	2
MALP-NE/Conv	-	-	2
Low Quality Conventional Concrete, Uncorroded Steel	-		
Conv-0.6wc	6	6	2*
MALP-E/Conv-0.6wc	3	3	2
Low Quality Conventional Concrete, Pre-Corroded Steel	-		
Conv-0.6wc-Corr	6	6	2*
MALP-E-Corr	3	3	2
MALP-E/Conv-0.6wc-Corr	3	3	2

\*One specimen with crack and one specimen without cracked

Notes: Conv = Conventional concrete; MALP-E = Magnesium–Aluminum–Liquid–Phosphate concrete with Endure; MALP-NE = Magnesium–Aluminum–Liquid–Phosphate concrete without Endure; MKP = Magnesium–Potassium–Phosphate-based concrete; MKP-VO = Magnesium–Potassium–Phosphate-based concrete for vertical/overhead applications; MALP-E/Conv = Composite specimen with half conventional concrete and half MALP with Endure; MALP-NE/Conv = Composite specimen with conventional concrete and MALP without Endure. Conv-0.6wc = Conventional concrete mixture with a water/cement ratio of 0.6. MALP-E/Conv-0.6wc = Composite specimen consisting of half Magnesium–Aluminum–Liquid–Phosphate concrete with Endure and half conventional concrete with a water/cement ratio of 0.6. Conv-0.6wc-Corr = Conventional concrete with a water/cement ratio of 0.6 containing pre-corroded reinforcement. MALP-E-Corr = Magnesium–Aluminum–Liquid–Phosphate concrete with Endure containing pre-corroded reinforcement. MALP-E/Conv-0.6wc-Corr = Composite specimen of half Magnesium–Aluminum–Liquid–Phosphate concrete with Endure and half conventional concrete with a water/cement ratio of 0.6, containing pre-corroded reinforcement.

## 2.5 Linear Polarization Resistance Measurements

Total corrosion, the sum of microcell and macrocell corrosion, for the beam and cracked beam specimens can be assessed using linear polarization resistance (LPR) measurements. This technique employs a non-corroding counter electrode and a reference electrode to generate a polarization curve by applying a series of potentials to the metal and recording the corresponding corrosion currents with a potentiostat. During testing, current measurements are collected through a gradual, short-range sweep of the bar potential. The typical sweep spans from -20 to +20 mV relative to the open-circuit potential, with the range from -10 to +10 mV

(where the current-voltage relationship is approximately linear) used for analysis. The slope of this linear region, expressed in  $\text{k}\Omega \cdot \text{cm}^2$  as  $R_p$ , reflects the metal's resistance. The total corrosion current density,  $i$ , in  $\text{A}/\text{cm}^2$ , is then calculated as shown in Eq. (2.2)

$$i = \frac{B}{R_p} \quad (2.2)$$

where  $B$  is the Stern-Geary constant, typically assumed to be 26 mV for corroding reinforcing steel in concrete. The total corrosion rate is expressed in  $\mu\text{m}/\text{year}$ . Linear polarization resistance (LPR) measurements are taken every four weeks to determine the total corrosion rates for the top mat bars, with the bottom mats disconnected. During the tests, the top mat of reinforcing steel serves as the working electrode, a saturated calomel electrode (SCE) immersed in the salt solution atop the specimen acts as the reference electrode, and a platinum strip, also immersed in the salt solution, functions as the counter electrode.

## 2.6 Freeze-thaw tests and scaling tests

The freeze-thaw resistance of the Phoscrete products, MALP and MKP, was evaluated following ASTM C666. Specimens were evaluated using both Procedure A (freezing and thawing in water) and Procedure B (freezing in air, thawing in water). Procedure A is the more aggressive of the two exposure conditions. Degradation of the concrete is evaluated using the relative dynamic modulus of elasticity, outlined in ASTM C215. Specimens are evaluated for a minimum of 600 cycles or until the relative dynamic modulus decreases to 60% of its initial value.

The freeze-thaw specimen is a prism,  $16 \times 3 \times 4$  in. ( $406 \times 76 \times 102$  mm), as shown in Fig. 2.11. Specimens consisted of monolithic MALP, with and without Endure, MKP and MKP-VO, along with specimens fabricated with conventional concrete with known freeze-thaw durability and MALP with Endure, as outlined in the test program in Table 2.4. MALP specimens with and without Endure, MKP, and MKP-VO specimens were cast for both procedures and finished the test. Vertical interface specimens were cast for Procedure B; however, because this type of specimen exhibited early failure in Procedure B, no corresponding specimens were prepared for Procedure A.

Fabrication:

Specimen fabrication for freeze-thaw specimens is as follows:

- 1- The metal forms were assembled and oiled prior to casting.
- 2- Specimens containing MALP with and without Endure, MKP, and MKP-VO were cast in a single layer, and the free surface of each specimen was finished with a trowel.
- 3- Specimens consisting of half MALP with Endure and half conventional concrete (horizontal interface) were cast in two layers. The conventional concrete (bottom side) was cast first. The specimens were demolded 24 hours after casting and cured in lime-saturated water for 28 days, followed by casting of the MALP layer on the upper side and finishing the free surface with a trowel.

4- The specimens were demolded immediately after the MALP had set and then cured for three days in an environmentally controlled room at a relative humidity of  $50 \pm 4\%$  and a temperature of  $73 \pm 3$  °F.

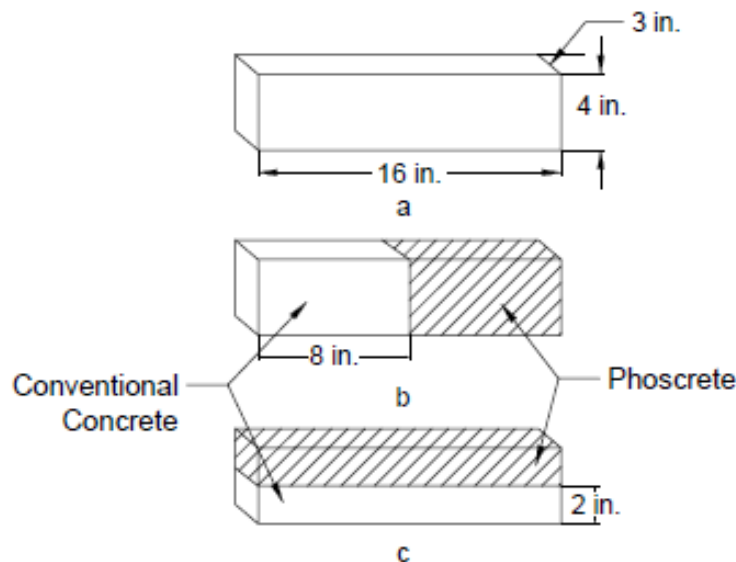


**Figure 2.11:** Freeze-thaw specimen, a) monolithic, b) vertical interface, c) horizontal interface

**Table 2.4:** Freeze-thaw test program

	Specimen Type		
	Monolithic	Vertical Interface*	Horizontal Interface*
ASTM C666 Procedure A		-	
MALP-E	3	3	3
MALP-NE	3	-	-
MKP	3	-	-
MKP-VO	3	-	-
ASTM C666 Procedure B		-	
MALP-E	3	3	3
MALP-NE	3	-	-
MKP	6	-	-
MKP-VO	3	-	-

\*Combined with conventional (Conv.) concrete

Notes: MALP-E = Magnesium–Aluminum–Liquid–Phosphate concrete with Endure; MALP-NE = Magnesium–Aluminum–Liquid–Phosphate concrete without Endure; MKP = Magnesium–Potassium–Phosphate-based concrete;

MKP-VO = Magnesium–Potassium–Phosphate-based concrete for vertical/overhead applications.

The scaling tests are performed in accordance with Quebec test BNQ NQ 2621-900 Annex B, with minor modifications to the temperature range for the freeze-thaw cycle. BNQ NQ 2621-900 uses a temperature of  $-0.4 \pm 5.4$  °F ( $-18 \pm 3$  °C) for the freezing period followed by a temperature of  $77 \pm 5.4$  °F ( $25 \pm 3$  °C) for the thawing period. The procedure specifies no limits on relative humidity (RH). In this study, the temperature was  $0 \pm 5$  °F ( $-18 \pm 3$  °C) during the freezing period and  $73 \pm 3$  °F ( $23 \pm 2$  °C) during the thawing period. During the thawing period, the RH was  $50\% \pm 4\%$ .

For the test, specimen dimensions are  $9 \times 16 \times 3$  in. (229 × 406 × 76 mm), cast in a single layer. The upper surface of the specimens is struck off with a wooden screed. The specimens are cured for 14 days and dried in an environmentally-controlled room at  $73 \pm 3$  °F ( $23 \pm 2$  °C) and a relative humidity of  $50\% \pm 4\%$  for 14 days. An expanded polystyrene dam is attached to the finished surface of the specimen. A  $\frac{1}{4}$ -in. deep layer of 3% NaCl solution is ponded within the dam to pre-saturate the specimens. The specimens are covered with a plastic sheet to prevent evaporation of the solution and stored for 7 days in an environmentally-controlled room a relative humidity of  $50 \pm 4\%$  and a temperature of  $73 \pm 3$  °F.

After the pre-saturation period, the specimens are exposed to cycles of freezing and thawing. Each cycle includes a  $16 \pm 1$  hr freezing phase followed by an  $8 \pm 1$  hr thawing phase. Mass loss in the specimens is measured after 7, 21, 35, and 56 cycles. To measure mass loss, lose material on the surface of the specimens is wet-sieved over a No. 200 (75 µm) sieve. The material retained on the No. 200 sieve is dried for approximately 24 hours at 212 °F. The total mass of material (including cumulative material lost from prior cycles) is then divided by the average surface area of the inside of the specimen to calculate the cumulative mass loss in terms of lb/ft<sup>2</sup>. New salt solution is added to specimens prior to returning them to testing. The maximum allowable average cumulative mass losses at the end of the test are 0.10 lb/ft<sup>2</sup> (500 g/m<sup>2</sup>) and 0.16 lb/ft<sup>2</sup> (800 g/m<sup>2</sup>) in accordance with Quebec Test BNQ NQ 2621-900 and the Ministry of Transportation of Ontario (MTO), respectively after 56 cycles. The test program is outlined in Table 2.5.

**Table 2.5:** Scaling test program

Specimen Type	Number of Specimens
MALP-E	6
MALP-NE	6
MKP	9
MKP-VO	3

Notes: MALP-E = Magnesium–Aluminum–Liquid–Phosphate concrete with Endure; MALP-NE = Magnesium–Aluminum–Liquid–Phosphate concrete without Endure; MKP = Magnesium–Potassium–Phosphate-based concrete; MKP-VO = Magnesium–Potassium–Phosphate-based concrete for vertical/overhead applications.

## 2.7 Shrinkage tests

Free shrinkage of MALP with and without Endure, MKP and MKO-VO specimens is measured using a modified version of ASTM C157. In the test, specimens with dimensions of  $3 \times 3 \times 11.25$  in. (76 × 76 × 286 mm) are cast in a single placement for each mixture to measure length change. Standard ASTM C157 test procedures call for demolding and initial specimen length measurements to be made  $23\frac{1}{2} \pm \frac{1}{2}$  hours after the addition of mixing water. MALP,

MKP and MKP-VO, however, are rapid-setting materials, and significant changes in volume occur during the first 24 hours that the standard test procedures do not capture. Instead, the specimens are demolded one half hour after mixing, with the exact time determined by a series of preliminary specimens used to determine the set time. Measurements begin immediately after demolding, with two more measurements at one-hour intervals on the first day, and continue once a week for 365 days in a controlled environment at a temperature of  $73^{\circ} \pm 3^{\circ}\text{F}$  ( $23^{\circ} \pm 2^{\circ}\text{C}$ ) and a relative humidity of  $50 \pm 4\%$ . The free shrinkage test program is outlined in Table 2.6.

In addition to free shrinkage measurements, crack width is monitored at the interface of the MALP or MKP and conventional reinforcement in the field test specimens described above to evaluate the effect of shrinkage at the interface of repairs.

**Table 2.6:** Free shrinkage test program

Specimen Type	Number of Specimens
MALP-E	12
MALP-NE	10
MKP	12
MKP-VO	5

Notes: MALP-E = Magnesium–Aluminum–Liquid–Phosphate concrete with Endure; MALP-NE = Magnesium–Aluminum–Liquid–Phosphate concrete without Endure; MKP = Magnesium–Potassium–Phosphate-based concrete; MKP-VO = Magnesium–Potassium–Phosphate-based concrete for vertical/overhead applications.

# CHAPTER 3: TEST RESULTS

## 3.1 Corrosion test results

The majority of the specimens listed in Table 2.3 reached 96 weeks in the corrosion tests, at which point they were removed from testing. Results for all specimens are presented in the sections that follow.

### 3.1.1 Beam and cracked beam specimens

Figure 3.1 shows the average macrocell corrosion rates for the beam specimens. Average corrosion potentials for the top mats of steel are shown in Figure 3.2, in which specimens with corrosion potentials more negative than  $-0.35$  V have greater than a 90 % probability that corrosion is occurring (ASTM C876).

As shown in Figure 3.1, the specimens with MKP exhibited active corrosion as early as six weeks, with average corrosion rates as high as  $20.9$   $\mu\text{m}/\text{yr}$  and corrosion potentials below  $-0.50$  V vs. CSE. Corrosion rates reached a high of  $20.9$   $\mu\text{m}/\text{year}$  at week 11, followed by a decrease to  $7.87$   $\mu\text{m}/\text{year}$  at week 31. From 33 weeks until the end of testing, the average corrosion rate for these specimens fluctuated around  $5$   $\mu\text{m}/\text{yr}$ . These specimens completed the 96-week test period. Specimens with the vertical/overhead placement formula of MKP (MKP-VO) exhibited low corrosion rates through eight weeks. The average corrosion rate of these specimens then increased to values similar to those of the standard MKP formulations until week 27, followed by a drop to around  $1$   $\mu\text{m}/\text{yr}$  through week 96.

Specimens with MALP without Endure (B-MALP-NE) exhibited a more negative corrosion potential (indicating a greater tendency to corrode) than those with Endure, but neither type of MALP specimen exhibited active corrosion, even when used in conjunction with conventional concrete (MALP/Conv) or with corroded reinforcement (B-MALP-E-Corr). Specimens containing MALP with and without Endure (B-MALP-E and B-MALP-NE) completed the 96-week test period and exhibited corrosion rates below  $1$   $\mu\text{m}/\text{yr}$  throughout the duration. Specimens consisting of half MALP and half conventional concrete (MALP/Conv) completed the 96-week test and exhibited corrosion rates close to zero throughout this period. Specimens containing MALP with Endure and corroded reinforcement (B-MALP-E-Corr) completed 95 weeks and also showed corrosion rates close to zero throughout the 95-week period. The conventional specimens (B-Conv) exhibited measurable corrosion but with corrosion rates below  $8$   $\mu\text{m}/\text{yr}$ . These specimens (B-Conv) completed the 96-week test period. These specimens exhibited a corrosion rate below  $3.5$   $\mu\text{m}/\text{yr}$  up to week 48. After week 48, the corrosion rate increased, exceeding  $5$   $\mu\text{m}/\text{yr}$  during most weeks to the end of test. The conventional specimens with low quality concrete (B-Conv-0.6wc) exhibited a corrosion rate as high as  $14.46$   $\mu\text{m}/\text{year}$  at week 31, followed by a steady decline to below  $5$   $\mu\text{m}/\text{year}$  at week 46. This was followed by an increase to  $11$   $\mu\text{m}/\text{year}$  at week 51, a subsequent drop to below  $5$   $\mu\text{m}/\text{year}$  at week 56, and another increase to above  $9.6$   $\mu\text{m}/\text{year}$  by week 79, and then a slight decrease to  $7.77$   $\mu\text{m}/\text{year}$  at week 84. The conventional specimens with low quality concrete and corroded bars (B-Conv-0.6wc-Corr) exhibited corrosion rates as high as  $27.9$   $\mu\text{m}/\text{yr}$  at week 24, followed by a steady decline, reaching approximately  $8$   $\mu\text{m}/\text{yr}$  at week 58. The corrosion rate then increased, reaching  $20.4$   $\mu\text{m}/\text{yr}$  by week 73 followed by a drop to  $16.1$   $\mu\text{m}/\text{yr}$  at week 78.

Specimens with half MALP with Endure in the upper layer of the specimens and half low-quality concrete in the lower layer (B-MALP-E/Conv-0.6wc) had corrosion rates close to zero by the end of week 72. Specimens with half MALP and half low-quality concrete with corroded reinforcement (B-MALP-E/Conv-0.6wc-Corr) also have corrosion rates below 1  $\mu\text{m}/\text{yr}$  through 67 weeks.

Overall, these results show that specimens containing MALP, both with and without Endure (MALP-E and MALP-NE), demonstrated excellent corrosion resistance, maintaining corrosion rates below 1  $\mu\text{m}/\text{yr}$  and stable corrosion potentials throughout the 96-week test period. Even when combined with conventional concrete (MALP-E/Conv) or pre-corroded reinforcement (MALP-E-Corr), MALP mixtures effectively protected the embedded steel, showing corrosion rates close to zero for the entire duration. In contrast, specimens containing MKP exhibited active corrosion as early as six weeks, with corrosion rates exceeding 20  $\mu\text{m}/\text{yr}$  and potentials below  $-0.50$  V vs. CSE, indicating a high probability of corrosion activity. Although the rates decreased over time, they remained significantly higher than those observed for MALP specimens. The MKP-VO formulation performed better than MKP, maintaining low corrosion rates for the first eight weeks and stabilizing near 1  $\mu\text{m}/\text{yr}$  after 27 weeks. The conventional concrete specimens (B-Conv) exhibited measurable corrosion throughout the 96 weeks, with rates typically below 8  $\mu\text{m}/\text{yr}$  but showing increasing activity after week 48. The low-quality concrete specimens (B-Conv-0.6wc) and low-quality corroded specimens (B-0.6wc-Corr) showed the most severe corrosion behavior, reaching rates as high as 27.9  $\mu\text{m}/\text{yr}$ . Specimens that incorporated MALP in combination with low-quality concrete (B-MALP-E/Conv-0.6wc and B-MALP-E/Conv-0.6wc-Corr) effectively suppressed corrosion, reducing rates to near zero by week 72 and below 1  $\mu\text{m}/\text{yr}$  through 67 weeks, respectively. These findings confirm that when the reinforcing bars are fully embedded in the repair materials, MALP-based systems provide superior long-term protection against corrosion compared to MKP and conventional concrete formulations.

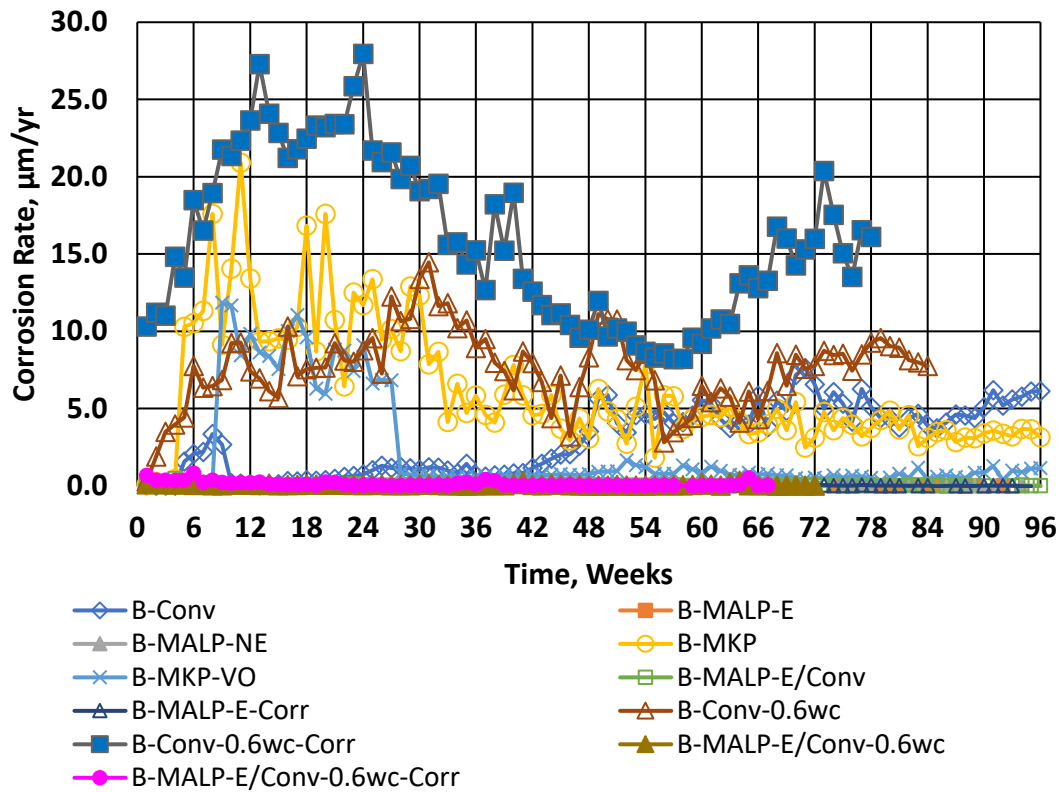


**Figure 3.1 – Average macrocell corrosion rates of specimens in the beam (B) test**

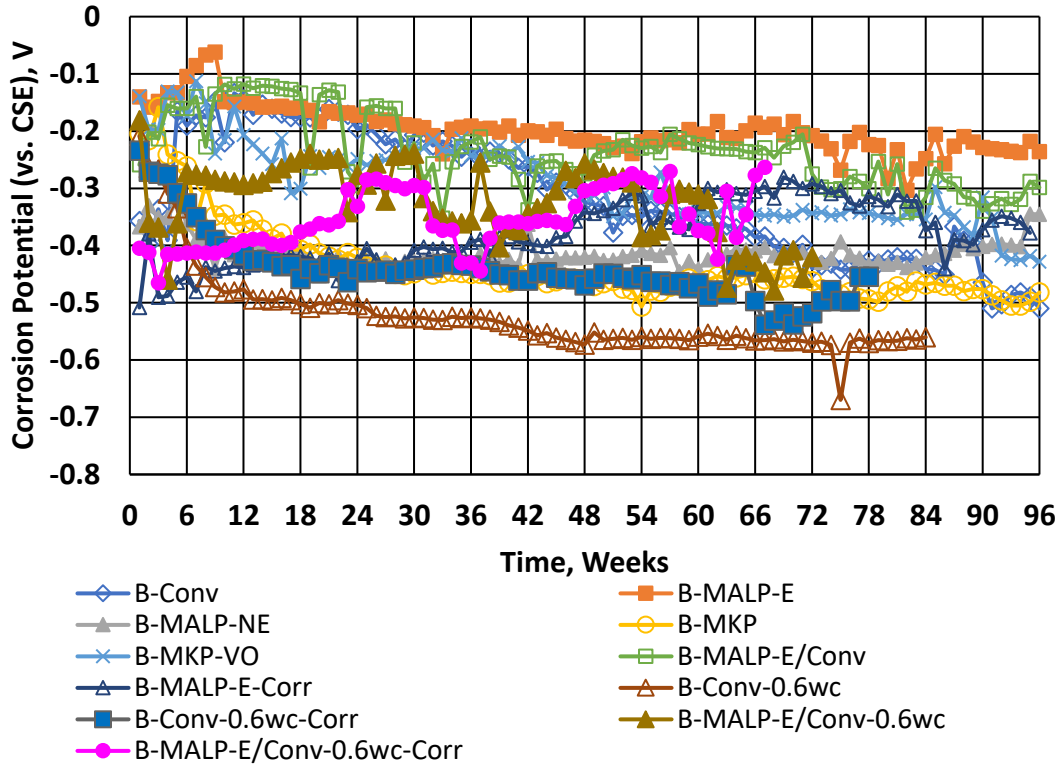


**Figure 3.2 – Average top mat corrosion potentials vs. CSE of specimens containing MALP and MKP in the beam (B) test**

Figure 3.3 shows the average macrocell corrosion rates for the cracked-beam specimens. Average corrosion potentials for the top mats of steel are presented in Figure 3.4. Specimens with corrosion potentials more negative than  $-0.35$  V have greater than a 90 % probability that corrosion is occurring (ASTM C876). As is the case in uncracked concrete, the specimens with MKP exhibited active corrosion, with corrosion rates as high as  $19$   $\mu\text{m}/\text{yr}$  and corrosion potentials below  $-0.50$  V vs. CSE, similar to the specimens with conventional concrete. These specimens (MKP) completed the 96-week test period. Like the beam specimens, the specimens with the vertical/overhead formulation of MKP (MKP-VO) initially showed low corrosion rates for about six weeks and then exhibited corrosion rates similar to the standard MKP formulation through 23 weeks, followed by a drop to less than  $3$   $\mu\text{m}/\text{yr}$ , continuing through 96 weeks.

Specimens with both MALP and conventional concrete (CB-MALP-E/Conv) exhibited low corrosion activity, occasionally with rates as high as  $1\text{--}2$   $\mu\text{m}/\text{yr}$ ; in most weeks, however, the rate remained close to zero. These specimens (CB-MALP-E/Conv) completed the 96-week test period. Other specimens consisting of MALP, both with and without Endure, did not exhibit active macrocell corrosion, but did exhibit similar corrosion potentials to those of the specimens with MKP. These specimens (CB-MALP-E and CB-MALP-NE) completed the 96-week test period.

The conventional concrete specimens (CB-Conv) exhibited an increase in corrosion rate up to week 15, reaching a peak value of  $17.3$   $\mu\text{m}/\text{year}$  at week 15, followed by a steady decline to  $3.1$   $\mu\text{m}/\text{year}$  at week 84, followed by an increase to  $8.2$   $\mu\text{m}/\text{yr}$  by the end of week 96.

Specimens with low quality concrete with corroded reinforcement (CB-Conv-0.6wc-Corr) exhibited corrosion rates above 20  $\mu\text{m}/\text{yr}$  most weeks through the end of week 74. Initially, these specimens exhibited a sharp increase in corrosion rates, reaching 33.2  $\mu\text{m}/\text{year}$  at week 9, followed by a gradual decline to 24.8  $\mu\text{m}/\text{year}$  at week 29, and a continued steady decrease to 10.6  $\mu\text{m}/\text{year}$  by week 57. Subsequently, a steady increase was observed, with the corrosion rate rising to 13.7  $\mu\text{m}/\text{year}$  at week 67. This was followed by a sharp increase reaching 25  $\mu\text{m}/\text{year}$  by the end of week 69. After that, these specimens (CB-Conv-0.6wc-Corr) exhibited fluctuations, reaching 20.3  $\mu\text{m}/\text{year}$  by week 78.

Specimens with low-quality concrete and uncorroded reinforcement (CB-Conv-0.6wc) exhibited an increase in corrosion rate up to week 25, reaching 22.5  $\mu\text{m}/\text{year}$ , followed by a steady decline to below 5  $\mu\text{m}/\text{year}$  by the end of week 67. These specimens (CB-Conv-0.6wc) exhibited a steady increase in corrosion rates, reaching 22.5  $\mu\text{m}/\text{year}$  at week 25. This was followed by a gradual decline to 10  $\mu\text{m}/\text{year}$  at week 55, after which a sharp drop was observed, with corrosion rates falling below 5  $\mu\text{m}/\text{year}$  at week 56 and reaching 5  $\mu\text{m}/\text{year}$  by week 84.

Specimens with MALP-E in the upper half of the specimens and low-quality concrete in the lower half, with and without corroded reinforcement (CB-MALP-E/Conv-0.6wc-Corr, CB-MALP-E/Conv-0.6wc) exhibited low corrosion rates, although the corrosion rates were greater than those for the same specimens with uncracked concrete. Both specimen types (CB-MALP-E/Conv-0.6wc-Corr and CB-MALP-E/Conv-0.6wc) exhibited corrosion rates below 3  $\mu\text{m}/\text{year}$  through weeks 67 and 72, respectively. Specimens with MALP and corroded reinforcement (CB-MALP-E-Corr) exhibited low corrosion rates, comparable to those of uncracked specimens, with values remaining close to zero throughout 95 weeks.

For the cracked-beam specimens, these results show that the presence of surface cracking accelerated corrosion activity in the conventional concrete and MKP-based systems but had minimal effect on MALP-based formulations. Specimens with MKP exhibited active corrosion similar to those in uncracked beams, with rates reaching up to 19  $\mu\text{m}/\text{yr}$  and corrosion potentials below  $-0.50$  V vs. CSE, confirming a high probability of corrosion. The MKP-VO specimens initially performed better, showing low corrosion rates during the first six weeks, but later exhibited corrosion behavior similar to standard MKP before stabilizing below 3  $\mu\text{m}/\text{yr}$  after week 23. Specimens containing MALP, both with and without Endure (CB-MALP-E and CB-MALP-NE), showed no evidence of active macrocell corrosion and maintained corrosion rates near zero through the 96-week test. Likewise, MALP combined with conventional concrete (CB-MALP-E/Conv) exhibited minimal corrosion activity, occasionally as high as 1–2  $\mu\text{m}/\text{yr}$  but generally close to zero, demonstrating the material's strong protective performance even under cracked conditions.

The conventional concrete specimens (CB-Conv) exhibited moderate to severe corrosion, with rates peaking at 17.3  $\mu\text{m}/\text{yr}$  at week 15 and fluctuating thereafter, while the low-quality concrete specimens (CB-Conv-0.6wc) and low-quality corroded specimens (CB-Conv-0.6wc-Corr) showed the highest corrosion rates, reaching 22–33  $\mu\text{m}/\text{yr}$  within the first 25 weeks before gradually declining. Specimens that incorporated MALP-E with low-quality concrete, with and without corroded reinforcement (CB-MALP-E/Conv-0.6wc-Corr and CB-MALP-E/Conv-0.6wc), also demonstrated superior corrosion resistance compared to conventional systems, maintaining rates below 3  $\mu\text{m}/\text{yr}$  through 67–72 weeks. Similarly, MALP with corroded reinforcement (CB-MALP-E-Corr) exhibited corrosion rates close to zero throughout the test period.

Overall, when the reinforcing bars were fully embedded in the repair materials, the MALP-based systems effectively controlled corrosion even in cracked conditions, significantly outperforming MKP and conventional concretes in terms of long-term durability and corrosion protection.

The corrosion rates shown in Figures 3.1 and 3.3 are macrocell corrosion rates, defined as corrosion where the anode and cathode are located far from each other. In this case, the anode is the top mat of steel and the cathode the bottom mat of steel. As explained in Section 1.2, corrosion can also occur in a localized manner, where the anode and cathode are close together, termed microcell corrosion. The sum of macrocell and microcell corrosion is referred to as total corrosion and is measured by linear polarization resistance (LPR).

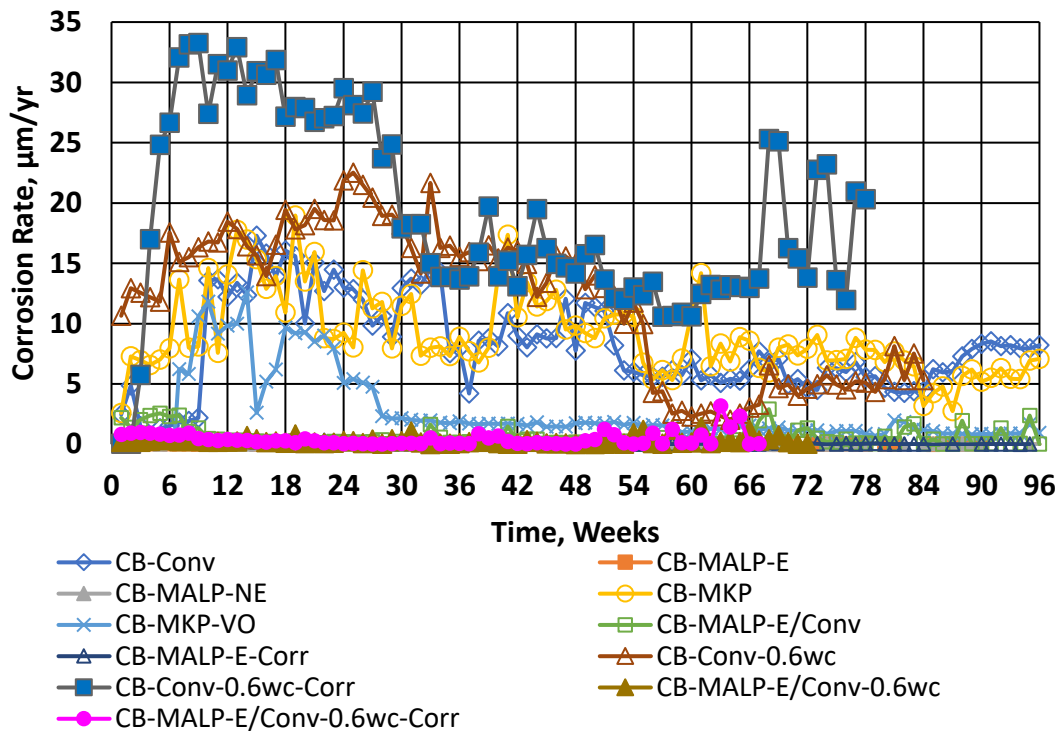


**Figure 3.3 – Average macrocell corrosion rates of specimens in the cracked-beam (CB) test**

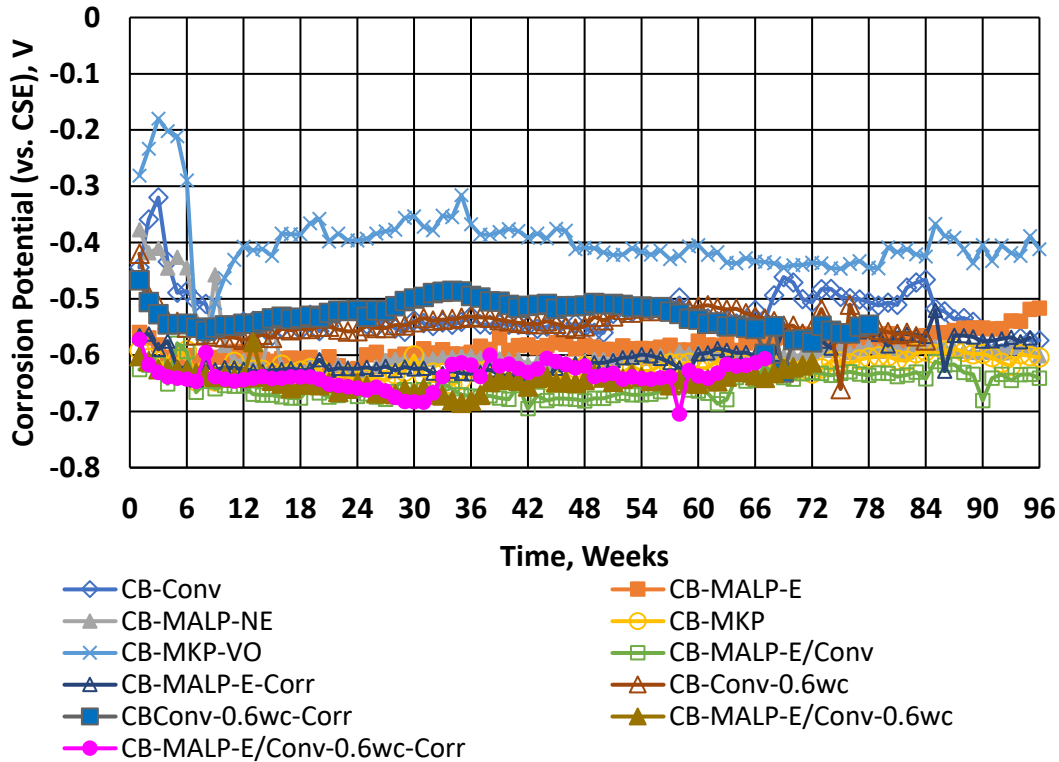


**Figure 3.4 – Average top mat corrosion potentials vs. CSE of specimens in the cracked-beam (CB) test**

Table 3.1 shows the macrocell and total corrosion losses for the Conv, MALP-E, MALP-NE, MKP, MKP-VO, MALP-E/Conv, MALP-E-Corr, Conv-0.6wc, and Conv-0.6wc-Corr, specimens, expressed in  $\mu\text{m}$ , which are obtained by integrating the corrosion rates shown in Fig. 3.1 and 3.3 over time. The table shows losses for all specimens that reached at least 76 weeks (all but two specimen types). Table 3.2 shows losses for the MALP/Conv-0.6wc and MALP/Conv-0.6wc-Corr specimens through week 64. As would be expected, because they include both macrocell and microcell losses, average total corrosion losses exceed average macrocell losses. The only exceptions are three uncracked specimen types with very low corrosion losses ( $\leq 0.15 \mu\text{m}$ ), MALP-E-Corr at week 76 and MALP/Conv-0.6wc and MALP/Conv-0.6wc-Corr at week 64. In these cases, it is likely that the small differences in the very low losses are due to variability in the low corrosion currents measured rather than statistically significant differences between macrocell and total corrosion.

Table 3.1 shows that the uncracked MALP specimens, with and without Endure (MALP-E and MALP-NE), exhibited minimal to no corrosion activity, with both macrocell and total corrosion losses in the range of 0 and  $0.02 \mu\text{m}$  through 76 weeks. Similarly, the uncracked specimens made with half MALP and half conventional concrete (MALP-E/Conv) showed a macrocell corrosion loss of  $0.05 \mu\text{m}$  and a total corrosion loss of  $0.19 \mu\text{m}$ . In contrast, the uncracked specimens composed of conventional concrete with a 0.6 w/c ratio and corroded reinforcement (Conv-0.6wc-Corr) displayed a macrocell loss of  $23.0 \mu\text{m}$  and a total corrosion loss of  $30.3 \mu\text{m}$ . The uncracked Conv.-0.6w/c specimens also exhibited elevated corrosion, with

a macrocell loss of 11.0  $\mu\text{m}$  and a total loss of 28.0  $\mu\text{m}$ . Generally, corrosion losses on the order of 25  $\mu\text{m}$  are enough to crack concrete with 1 in. cover (Darwin et al. 2011, O'Reilly et al. 2011).

The uncracked MKP and MKP-VO specimens had moderate corrosion activity, with macrocell losses of 8.53 and 3.87  $\mu\text{m}$  and total corrosion losses of 14.9 and 10.3  $\mu\text{m}$ , respectively. The uncracked specimens containing conventional concrete (Conv) demonstrated a macrocell corrosion loss of 3.59  $\mu\text{m}$ , with a corresponding total corrosion loss of 5.85  $\mu\text{m}$ .

In the cracked specimens, those containing MALP-E and MALP-NE showed relatively low macrocell corrosion losses of 0.01 and 0.02  $\mu\text{m}$ , and total corrosion losses of 2.45 and 4.50  $\mu\text{m}$ , respectively. That total losses are much higher relative to the macrocell losses can be explained by microcell corrosion and localized anodic activity, which cause additional steel loss not captured by macrocell measurements. Specimens containing MALP with corroded reinforcement (MALP-E-Corr) showed a macrocell corrosion loss of just 0.18  $\mu\text{m}$  but a high total corrosion loss of 22.0  $\mu\text{m}$ . The MALP-E/Conv specimens showed a macrocell corrosion loss of 0.59  $\mu\text{m}$  and a total corrosion loss of 20.1  $\mu\text{m}$ . As would be expected, the cracked specimens with conventional concrete with a 0.6 w/c ratio and corroded reinforcement (Conv-0.6wc-Corr) demonstrated high corrosion losses, with a macrocell corrosion loss of 27.2  $\mu\text{m}$  and a high total corrosion loss of 41.77  $\mu\text{m}$ . Similarly, Conv-0.6w/c specimens showed a macrocell corrosion loss of 18.4  $\mu\text{m}$  and a total loss of 33.0  $\mu\text{m}$ . The MKP specimens exhibited high corrosion activity, with a macrocell corrosion loss of 14.4  $\mu\text{m}$  and a total corrosion loss of 31.9  $\mu\text{m}$ , while MKP-VO specimens showed a macrocell loss of 4.17  $\mu\text{m}$  and a total corrosion loss of 4.87  $\mu\text{m}$ . Specimens composed of conventional concrete (Conv) exhibited a macrocell corrosion loss of 12.6  $\mu\text{m}$  and a corresponding total corrosion loss of 19.0  $\mu\text{m}$ .

**Table 3.1 – Average macrocell and total corrosion losses at week 76**

-	Uncracked	Uncracked	Cracked	Cracked
-	Macrocell Loss ( $\mu\text{m}$ )	Total Loss ( $\mu\text{m}$ )	Macrocell Loss ( $\mu\text{m}$ )	Total Loss ( $\mu\text{m}$ )
<b>Conv.</b>	3.59	5.85	12.6	19.0
<b>MALP-E</b>	0.01	0.00	0.01	2.45
<b>MALP-NE</b>	0.02	0.02	0.02	4.50
<b>MKP</b>	8.53	14.9	14.4	31.9
<b>MKP-VO</b>	3.87	10.3	4.17	4.87
<b>MALP-E/Conv</b>	0.05	0.19	0.59	20.1
<b>MALP-E-Corr</b>	0.06	0.01	0.18	22.0
<b>Conv.-0.6wc</b>	11.0	28.0	18.4	33.0
<b>Conv.-0.6wc-Corr</b>	23.0	30.3	27.2	41.8

**Table 3.2 – Average macrocell and total corrosion losses at week 64**

-	Uncracked	Uncracked	Cracked	Cracked
-	Macrocell Loss ( $\mu\text{m}$ )	Total Loss ( $\mu\text{m}$ )	Macrocell Loss ( $\mu\text{m}$ )	Total Loss ( $\mu\text{m}$ )
<b>MALP-E/Conv-0.6wc</b>	0.08	0.03	0.33	41.2
<b>MALP-E/Conv-0.6wc-Corr</b>	0.15	0.02	0.49	31.2

Table 3.2 compares the average macrocell corrosion losses with the average total corrosion losses at week 64 for specimens with MALP with Endure in the upper half and low-quality concrete in the lower half with and without corroded reinforcement, MALP-E/Conv-0.6wc and MALP-E/Conv-0.6wc-Corr, respectively. At week 64, the cracked specimens composed of MALP-E/Conv-0.6wc with and without corroded reinforcement exhibited macrocell corrosion losses of 0.49 and 0.33  $\mu\text{m}/\text{year}$ , and total corrosion losses of 31.2 and 41.2  $\mu\text{m}/\text{year}$ , respectively. Uncracked specimens are not showing significant corrosion activity. The large difference in macrocell and total corrosion for the specimens in the cracked beam test suggests a large amount of localized corrosion activity.

The LPR results provide an excellent picture of the behavior of the products under study and the degree to which they protect reinforcing steel concrete from corrosion, demonstrating that MALP, particularly MALP with Endure, offer excellent corrosion resistance compared to MKP and conventional concrete. The data indicate that MALP mixtures, whether used alone, in combination with conventional concrete, or with corroded reinforcement, maintained extremely low macrocell and total corrosion losses through the test duration, even under cracked conditions. In contrast, MKP and conventional concrete exhibited significantly higher corrosion losses, especially in cracked and low-quality concrete specimens, confirming that the MALP formulation provide the most effective long-term protection for embedded steel reinforcement. MKP-VO performed significantly better than MKP, but as well as MALP.

Figure 3.5 shows representative beam specimens incorporating MALP, both with and without Endure (MALP-E and MALP-NE), after 96 weeks of exposure. Figure 3.6 shows upper reinforcing bars from the same specimens. No visible corrosion products were observable on the exterior surfaces of the specimens (Figure 3.5), and signs of corrosion on the bars were restricted to localized areas with small rust patches. Overall, based on the results and autopsy of the reinforcement, MALP with or without Endure is effective in limiting the progression of corrosion of steel reinforcement when it completely encloses the bars. This protection is likely due to the very low permeability of MALP, an observation that is supported by the very low macrocell corrosion rates and losses observed for specimens with simulated cracks above the top bars, as well as the MALP-E and MALP-NE specimens without a simulated crack.

Figure 3.7 shows cracked beam specimens containing MALP with and without Endure (MALP-E and MALP-NE) at the end of 96-week test. Figure 3.8 shows the upper steel bars from

cracked beam MALP specimens with and without Endure after 96 weeks. There is no sign of corrosion on the outside of the specimens (Figure 3.7) and corrosion on the bars is limited to localized spots with visible patches of rust. Even in the presence of cracks, MALP concrete with and without Endure has provided a good level of protection, limiting extensive corrosion in reinforced bars, when the material encases all reinforcement.

Figure 3.9 shows beam specimens containing MKP and MKP-VO after 96 weeks of exposure, while Figure 3.10 shows the upper steel bars from these specimens. In the MKP specimens, corrosion products were not evident on the upper exterior surfaces (Figure 3.9a), but did have rust evident on the concrete at the end of the of the specimens and had rust patches distributed over the steel bar (especially at the end). While the MKP-VO specimens displayed no corrosion products on the exterior surfaces (Figure 3.9b), and the observed corrosion was uniformly distributed over the steel bar. Overall, the results and autopsy images indicate that MKP-VO concrete provided superior protective performance in beam specimens compared to MKP concrete, but less than that of MALP.

Figure 3.11 shows cracked beam specimens containing MKP and MKP-VO after 96 weeks of exposure, and Figure 3.12 shows the upper steel bars from these specimens. Corrosion products were observed on the exterior surfaces at the cracks of both MKP and MKP-VO specimens (Figures 3.11a and 3.11b). In the bars in the MKP specimens, the corrosion products rust were spread over wider areas, whereas in the MKP-VO specimens, corrosion was restricted to smaller, localized spots (Figure 3.12). Overall, the results and autopsy images demonstrate that MKP-VO concrete was more protective than MKP concrete in the cracked beam specimens, but less so than MALP-E or MALP-NE.



**Figure 3.5a –** MALP beam specimen with Endure (MALP-E)



**Figure 3.5b –** MALP beam specimen without Endure (MALP-NE)

**Figure 3.5 –** MALP beam specimens with and without Endure at 96 weeks



**Figure 3.6a** – Upper steel bar from MALP beam specimens with Endure



**Figure 3.6b** – Upper steel bar from MALP beam specimens without Endure

**Figure 3.6** – Top mat steel bars from MALP beam specimens with and without Endure at 96 weeks



**Figure 3.7a** – MALP cracked beam specimen with Endure



**Figure 3.7b** – MALP cracked beam specimen without Endure

**Figure 3.7** – Cracked beam specimens with and without Endure at 96 weeks



**Figure 3.8a** – Upper steel bar from MALP cracked beam specimens with Endure



**Figure 3.8b** – Upper steel bar from MALP cracked beam specimens without Endure

**Figure 3.8** – Top mat steel bars from MALP cracked beam specimens with and without Endure at 96 weeks



**Figure 3.9a** – MKP beam specimen



**Figure 3.9b** – MKP-VO beam specimen

**Figure 3.9** – MKP and MKP-VO beam specimens at 96 weeks



**Figure 3.10a** – Upper steel bar from MKP beam specimen



**Figure 3.10b** – Upper steel bar from MKP-VO beam specimen

**Figure 3.10** – Top mat steel bars from MKP and MKP-VO beam specimens at 96 weeks



**Figure 3.11a** – MKP cracked beam specimen



**Figure 3.11b** – MKP-VO cracked beam specimen

**Figure 3.11** – MKP and MKP-VO cracked beam specimens at 96 weeks



**Figure 3.12a** – Upper steel bar from MKP cracked beam specimen



**Figure 3.12b** – Upper steel bar from MKP-VO cracked beam specimen

**Figure 3.12** – Top mat steel bars from MKP and MKP-VO cracked beam specimens at 96 weeks

### 3.1.2 Field test specimens

Figure 3.13(a) shows the average macrocell corrosion rates for the field test specimens. The average corrosion potentials for the top mats of steel are shown in Figure 3.14(a), which indicates that at some time during the tests, all specimens exhibited a corrosion potential more negative than  $-0.35$  V and were, thus, likely undergoing active corrosion.

As shown in Figure 3.13(a), corrosion rates are about one order of magnitude lower than those exhibited by the beam and cracked beam specimens. This is expected based on both the differences in exposure conditions and specimen configuration.

The specimens with low-quality concrete and pre-corroded reinforcement (MALP-E-A-Conv-0.6wc-Corr and MALP-E-B-Conv-0.6wc-Corr) exhibited average corrosion rates as high as 7.17 and 5.21  $\mu\text{m}/\text{yr}$ , respectively, and corrosion potentials more negative than  $-0.35$  V vs. CSE. The specimens containing conventional concrete, both without and with simulated cracks (Conv-Uncracked, Conv-Cracked), have average corrosion rates below 2  $\mu\text{m}/\text{yr}$  after sixteen months. The specimens containing conventional concrete with repair patches, including MALP with and without Endure and the edges of the repair patch perpendicular to the bars in the upper layer (MALP-E-B-Conv and MALP-NE-B-Conv), exhibited active corrosion, with average corrosion rates as high as 2.46 and 2.5  $\mu\text{m}/\text{yr}$ , respectively. Specimens containing low-quality concrete with edges of the MALP repair patches perpendicular to the bars in the upper layer and with the edges aligned directly above the reinforcement (MALP-E-B-Conv-0.6wc, MALP-E-A-Conv-0.6wc), respectively, exhibited corrosion rates as high as 2.81 and 1.64  $\mu\text{m}/\text{yr}$ . The cracked and uncracked MALP field test specimens (consisting entirely of MALP), both with and without corroded reinforcement, demonstrated low corrosion rates, below 0.2  $\mu\text{m}/\text{yr}$ , during the

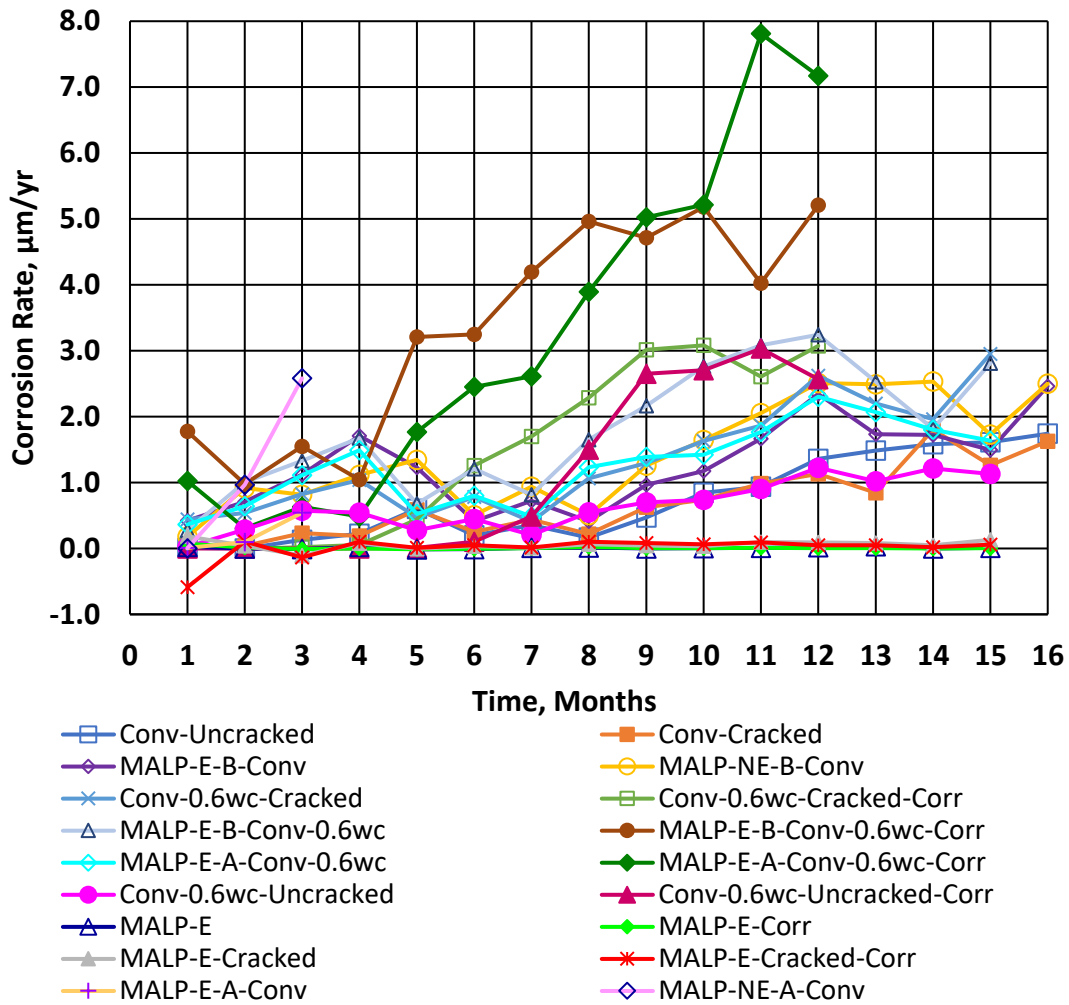
15-month test period. Specimens consisting of low-quality concrete with cracks (Conv-0.6wc-Cracked) exhibited average corrosion rates of 2.95  $\mu\text{m}/\text{year}$  during the 15-month period, while those without cracks (Conv-0.6wc-Uncracked) had average corrosion rates of 1.13  $\mu\text{m}/\text{year}$  during the same period. Specimens with low-quality concrete, cracks, and pre-corroded reinforcement (Conv-0.6wc-Cracked-Corr) exhibited average corrosion rates close to zero for the first four months, followed by an increase to 3.08  $\mu\text{m}/\text{year}$  at month 10, followed by a drop to 2.61  $\mu\text{m}/\text{year}$  at month 11, and then an increase to 3.07  $\mu\text{m}/\text{year}$  at month 12. In contrast, the specimens with low-quality concrete, no cracks, and pre-corroded reinforcement (Conv-0.6wc-Uncracked-Corr) maintained corrosion rates close to zero for six months before increasing to 3.03  $\mu\text{m}/\text{year}$  at month 11, followed by a drop to 2.57  $\mu\text{m}/\text{year}$  at month 12. The specimens containing conventional concrete with reinforcement that had not been pre-corroded with repair patches, including MALP with and without Endure and the edges of the repair patch aligned directly above the reinforcement (MALP-E-A-Conv and MALP-NE-A-Conv) exhibited average corrosion rates 0.54 and 2.58  $\mu\text{m}/\text{year}$ , respectively, after a shortened test period of 3 months.

The field test specimen data clearly demonstrate that corrosion behavior depends on both concrete quality and repair configuration. Specimens made entirely of MALP, with or without Endure (MALP-E and MALP-NE), maintained corrosion rates below 0.2  $\mu\text{m}/\text{yr}$  throughout the test, confirming their superior protective capability even in field conditions. The low-quality concrete specimens (0.6 w/c) with MALP repair regions exhibited higher and more variable corrosion rates, particularly when combined with corroded reinforcement, where peaks of 5–7  $\mu\text{m}/\text{yr}$  were recorded near month 12. For the conventional concrete specimens, both cracked and uncracked, corrosion rates remained relatively low (below 2  $\mu\text{m}/\text{yr}$ ) through 16 months, while the MALP-Conv repair specimens showed moderate corrosion depending on patch edge orientation. The specimens with patch edges aligned directly above the reinforcement (A type in title), MALP-E-A-Conv and MALP-NE-A-Conv, showed slightly higher initial corrosion rates (up to 2.58  $\mu\text{m}/\text{yr}$ ) than those with edges located between reinforcing bars (B type in title), where corrosion remained near 2.5  $\mu\text{m}/\text{yr}$  or less. This difference suggests that when the patch boundary lies directly over a bar, moisture and oxygen ingress along the steel interface are more likely to result in corrosion initiation.

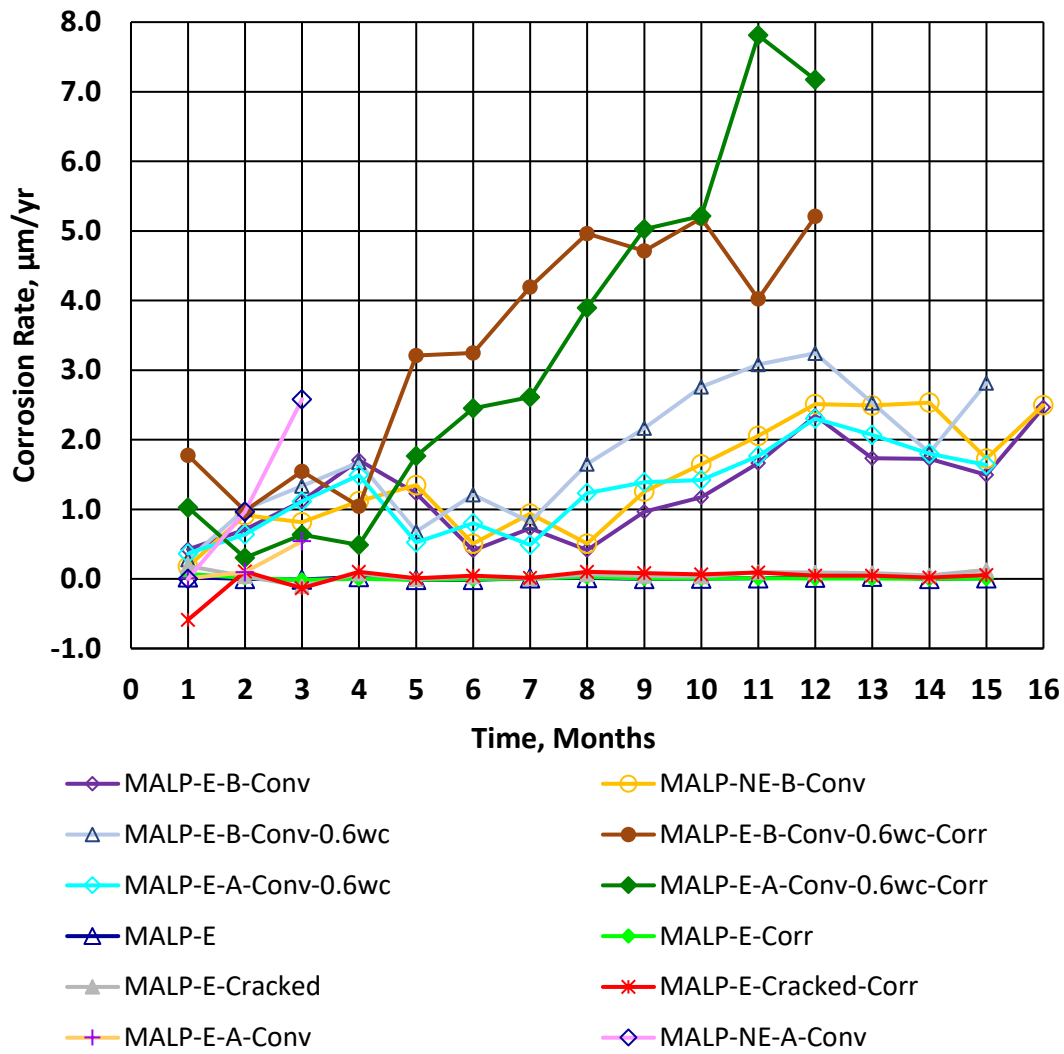
Overall, the results indicate that edge alignment and substrate quality are key factors controlling repair performance. Cracks and bar-aligned patch edges increase the likelihood of localized corrosion, whereas MALP based repairs that provide no access to deicing chemicals substantially reduce corrosion activity and provide durable protection to the embedded reinforcement.

Figure 3.13(b) highlights the corrosion performance of the MALP-based specimens only. The specimens made entirely of MALP, with Endure and regardless of cracking or reinforcement condition, maintained very low corrosion rates (below 0.2  $\mu\text{m}/\text{yr}$ ) throughout the test, demonstrating excellent field durability. MALP repair patches placed over conventional concrete showed moderate corrosion activity, generally below 2.5  $\mu\text{m}/\text{yr}$ , with slightly higher rates when patch edges were aligned directly above reinforcing bars (A-type). In the most severe configuration, low-quality substrate concrete combined with pre-corroded reinforcement, MALP repair regions exhibited higher peaks (5–7  $\mu\text{m}/\text{yr}$  near month 12), indicating that substrate quality and reinforcement condition significantly affect performance. Overall, MALP systems provided the most stable and lowest corrosion rates among all field specimens. Figure 3.14(b) shows that all MALP-based specimens exhibited corrosion potentials more negative

than  $-0.35$  V vs. CSE during the test period, indicating active corrosion conditions across all configurations. Despite these negative potentials, the MALP only specimens (with Endure and with or without cracks) maintained very low corrosion rates, confirming that their corrosion activity remained minimal even when potentials suggested otherwise.



**Figure 3.13(a) – Average macrocell corrosion rates of field test specimens**



**Figure 3.13(b)** – Average macrocell corrosion rates for field test specimens incorporating MALP

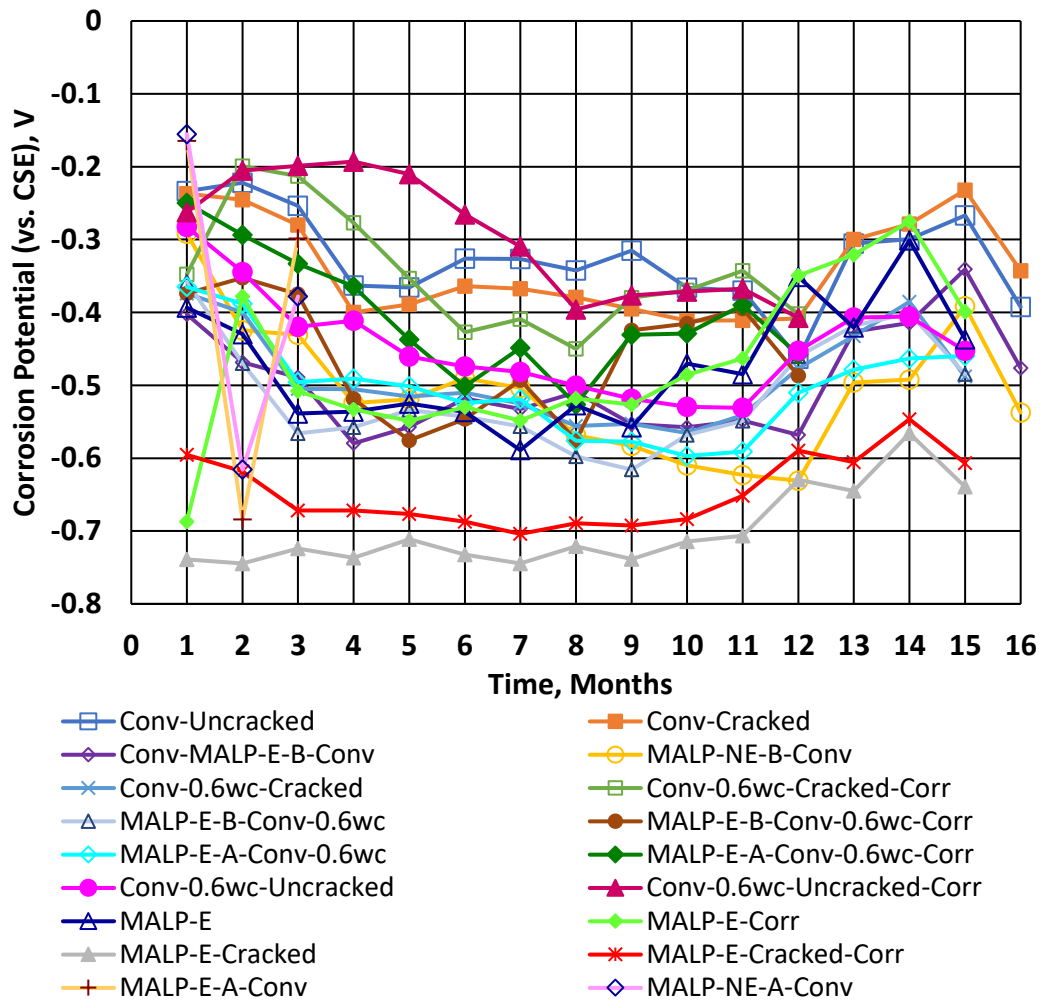


**Figure 3.14(a)** – Average top mat corrosion potentials vs. CSE of field test specimens

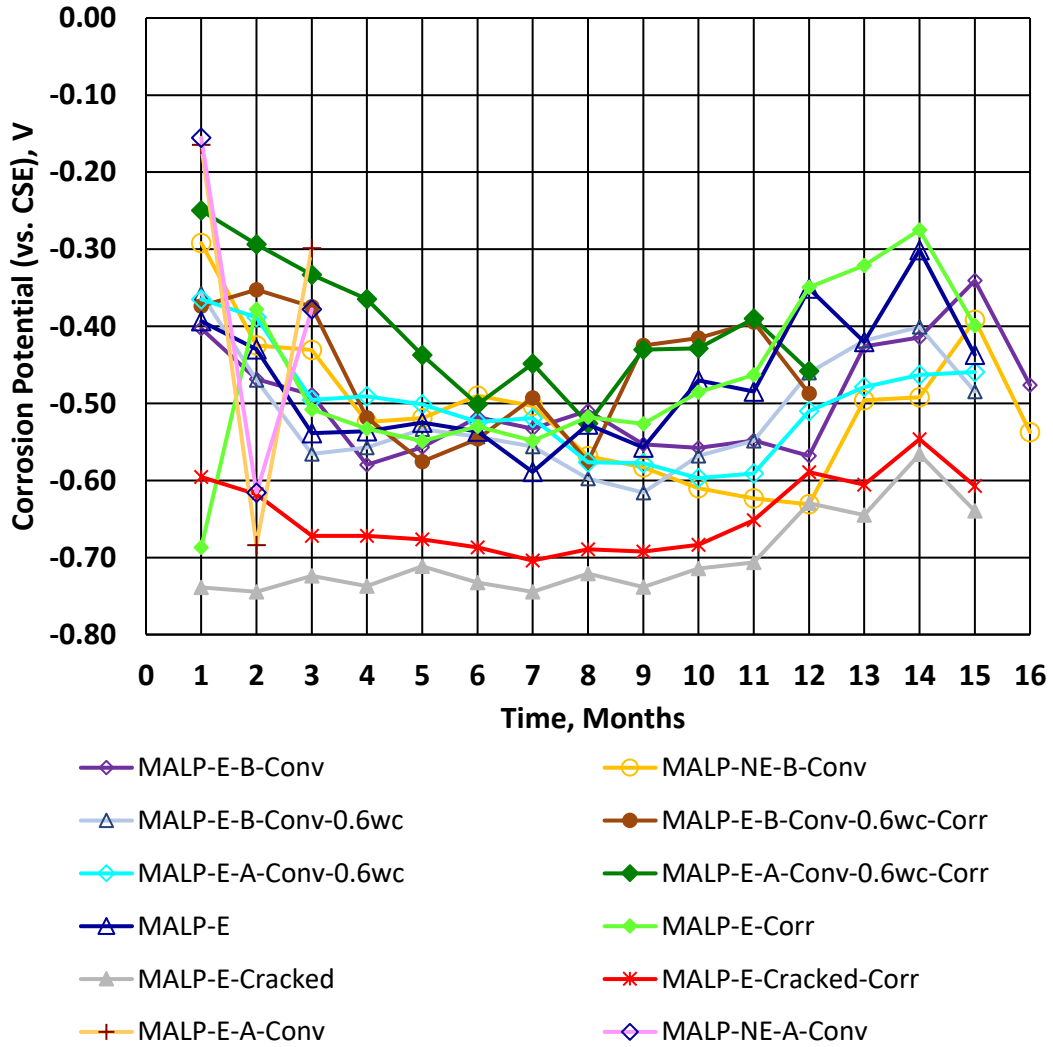


**Figure 3.14(b) – Average top mat corrosion potentials vs. CSE of field test specimens incorporating MALP**

### 3.2 Freeze-thaw and scaling test results

**Freeze-thaw:** Figure 3.15 shows the average percentage of the initial dynamic modulus of elasticity versus the number of cycles for specimens evaluated using Procedure A of ASTM C666 (freezing and thawing in water), along with the failure limit of 90% of the initial dynamic modulus of elasticity that is typically used for this test. Specimens that sustain a value of  $E_{dyn}$  above 90% of the initial value for at least 300 cycles are generally considered to represent durable concrete. Six specimens containing MALP, three each with and without Endure, three MKP specimens, three MKP-VO specimens, and three MALP-E/Conv (horizontal interface) were tested. Both MALP specimen types (MALP-E and MALP-NE) exhibited increases in initial dynamic modulus of elasticity, reaching 140% and 150% of their initial dynamic modulus of elasticity for much of the test period, respectively. These specimens passed more than 1000 cycles without any signs of

cracking or deterioration based on the percentage of the initial dynamic modulus of elasticity  $E_{dyn}$ . In contrast, the MKP specimens exhibited a sharp drop in the dynamic modulus of elasticity, reaching 60% of the initial value after just 163 cycles. The MKP-VO specimens, with a lower relative value of  $E_{dyn}$  than the MALP specimens, nevertheless exhibited no drop in  $E_{dyn}$  through 500 cycles, after which  $E_{dyn}$  began to decrease, reaching 90% after 675 cycles and 63% after 1019 cycles. The three MALP-E/Conv specimens (horizontal interface) exhibited an increase in dynamic modulus through the first 56 cycles followed by a slow drop to 90% after 706 cycles and 76% after 1004 cycles.

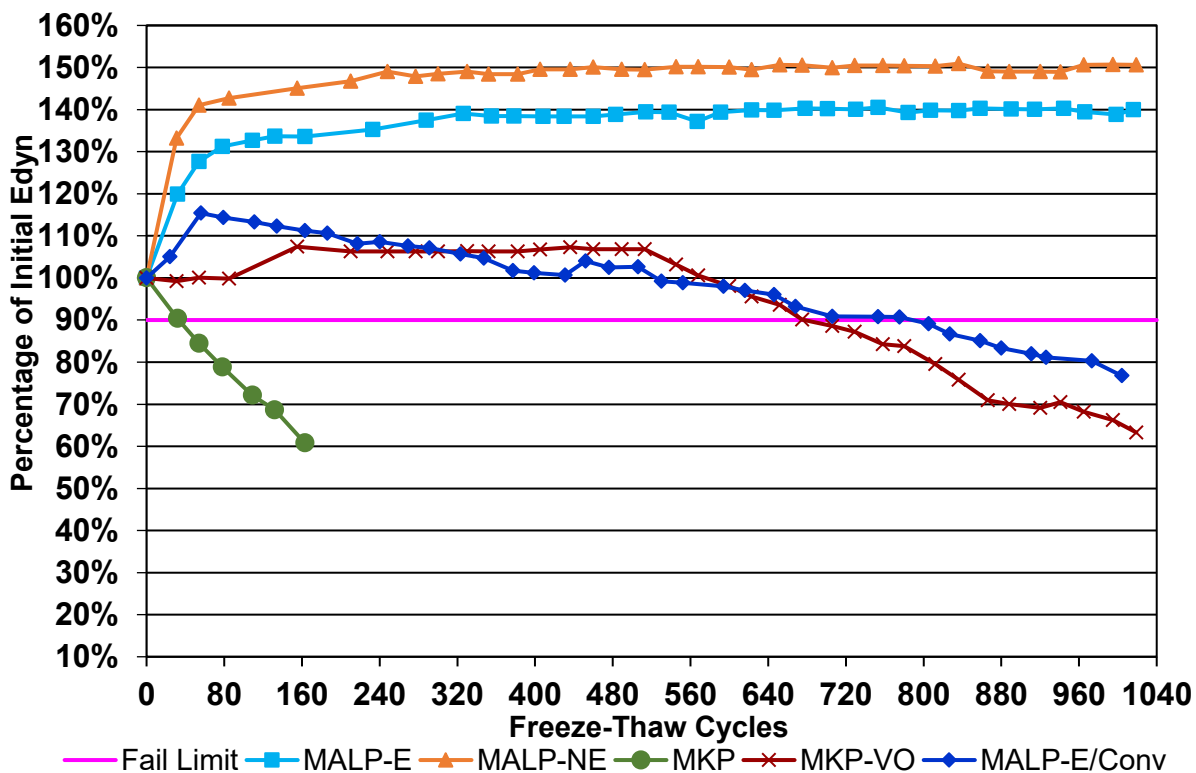


**Figure 3.15 – Percentage of initial dynamic modulus of elasticity vs. number of freeze-thaw cycles under ASTM C666 Procedure A**

Six specimens containing MALP, three with and three without Endure (MALP-E and MALP-NE), three specimens each with MKP and MKP-VO, and three MALP-E/Conv specimens were tested in accordance with ASTM C666 Procedure B (freezing in air and thawing in water). Figure 3.16 shows the average percentage of the initial dynamic modulus of elasticity versus the number of cycles, along with the failure limit of 95% of the initial dynamic modulus of elasticity that is typically used for this test. The first set of specimens with MKP (MKP-1) exhibited a steady drop in relative dynamic modulus throughout testing, reaching the 95% failure threshold in as few as 30 cycles (average of 25 cycles) and 60% of the initial dynamic modulus at an average of 338 cycles. Testing has continued to obtain additional data. Two of the three specimens have a single horizontal crack, which first appeared after about 750 cycles (Figure 3.17). To verify this performance, three more MKP specimens were cast (MKP-2). The recast

specimens reached the 95% failure limit at an average of 27 cycles and 60% of the initial dynamic modulus at an average of 199 cycles, similar to the performance of the initial specimens. Both types of MALP specimens exhibited increases in relative dynamic modulus throughout testing, reaching 1031 freeze-thaw cycles without any signs of deterioration. The three MKP-VO specimens maintained a constant modulus of 95% of the initial dynamic modulus for 249 cycles. Thereafter, the modulus began to steadily decrease, reaching 90% of the initial value after 359 cycles, followed by a decline to 60% of the initial modulus after 632 cycles. The three MALP-E/Conv (horizontal interface) specimens showed increases in relative dynamic modulus through 57 cycles, followed by a steady drop to 56% at approximately 289 cycles. MALP-E/Conv (vertical interface) specimens broke at the interface soon after initiation of testing and are not shown.

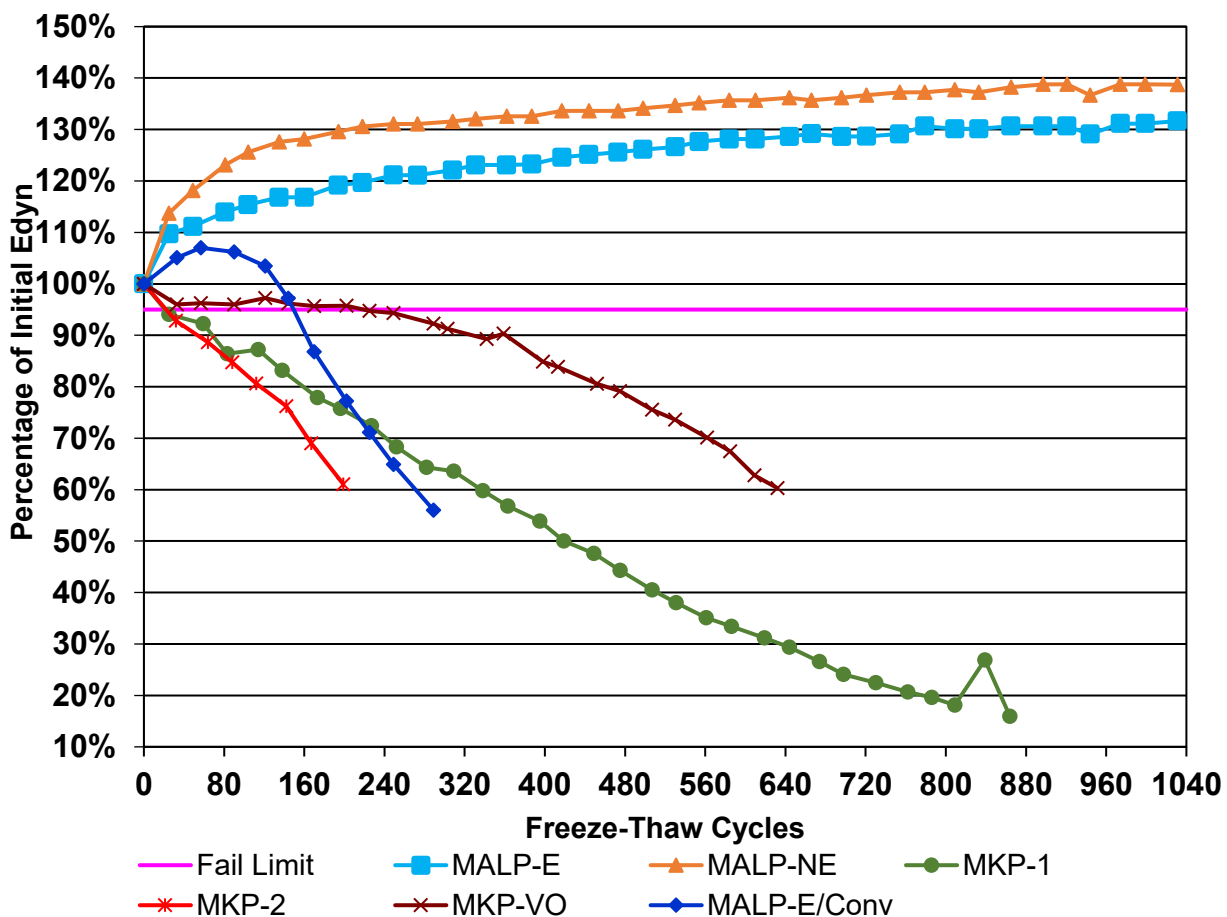


**Figure 3.16-** Percentage of initial dynamic modulus of elasticity vs. number of freeze-thaw cycles under ASTM C666 Procedure B

The freeze-thaw results based on Procedures A and B demonstrate that MALP, both with and without Endure, exhibits outstanding durability, showing significant increases in relative dynamic modulus of elasticity and no signs of deterioration even after more than 1000 cycles. This behavior indicates that MALP concretes possess an exceptionally stable microstructure and strong resistance to freeze-thaw damage. In contrast, MKP and MKP-VO has much lower

resistance. Under Procedure A, the MKP specimens lost nearly 40% of their initial modulus after only 163 cycles, while MKP-VO exhibited gradual deterioration after 500 cycles, reaching 63% of the initial modulus at 1019 cycles. The poor performance of MKP under Procedure B, with failure occurring within the first 30 cycles, further confirms its limited freeze-thaw resistance. The MALP-E/Conv composite specimens performed moderately well: they initially gained stiffness but gradually declined to about 76% of their initial modulus after 1000 cycles under Procedure A, and to 56% after 289 cycles under Procedure B. These results indicate that the bond at the MALP and conventional concrete interface, bond that may have been reduced under the cyclic wetting and drying that can occur to some degree under procedure B, is a critical factor influencing long term freeze-thaw durability.

Overall, these findings confirm that MALP products, especially when used monolithically, provide superior freeze-thaw resistance compared with MKP, while interfaces between MALP and conventional concrete may be vulnerable under severe cyclic exposure.



**Figure 3.17-** Three MKP specimens after 864 cycles (Procedure B) in freeze-thaw testing

**Scaling:** In the scaling test, six MALP specimens with Endure (MALP-E), six MALP specimens without Endure (MALP-NE), nine MKP specimens, and nine MKP-VO specimens were tested. Average results for all specimens are shown in Figure 3.18. Specimens containing MALP without Endure exhibit a significantly higher rate of average mass loss compared to those with Endure. Both types of MALP specimen exhibit mass losses that exceed the maximum allowable average cumulative mass losses at the end of the test of  $0.10 \text{ lb}/\text{ft}^2$  and  $0.16 \text{ lb}/\text{ft}^2$  in accordance with Quebec Test BNQ NQ 2621-900 and the Ministry of Transportation of Ontario

(MTO), respectively. The MKP and MKP-VO specimens demonstrate an average mass loss close to zero after 56 cycles.

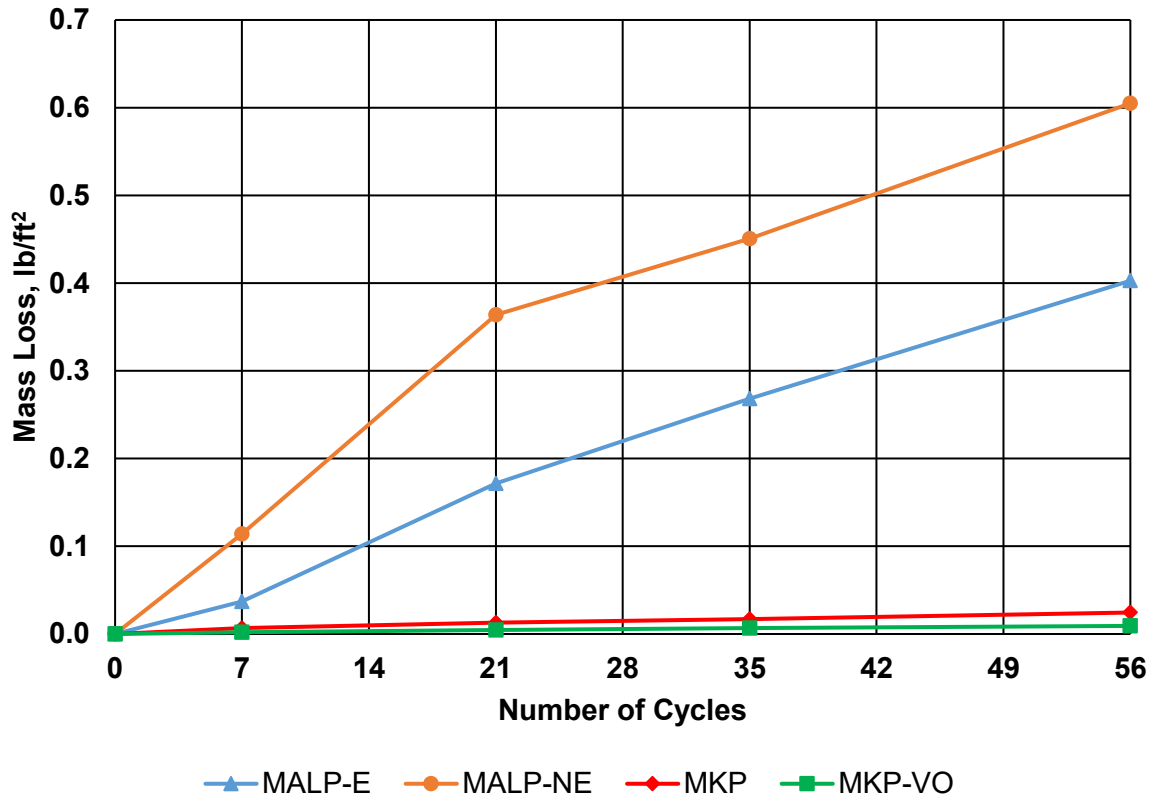


**Figure 3.18-** Average mass loss per  $\text{ft}^2$  vs. number of cycles in the scaling test

### 3.3 Shrinkage test results

In the shrinkage tests, 12 MALP specimens with Endure (MALP-E), 10 MALP specimens without Endure (MALP-NE), 12 MKP specimens, and five MKP-VO specimens were tested. Figure 3.19 shows the average values of strain as a function of time after casting. Negative values indicate shrinkage and positive values indicate expansion. Beginning early in the test, the MALP-E, MALP-NE, and MKP-VO specimens shrank, while the MKP specimens expanded. There was no sign of early expansion of MALP, as had been indicated by Floyd et al. (2021). The specimens containing MALP without Endure exhibited greater shrinkage than those with Endure throughout the test, but both shrank more than 500 microstrain over the course of the test. The MKP-VO specimens exhibited lower shrinkage than the MALP with Endure (MALP-E) specimens throughout 295 days. In contrast, the MKP specimens expanded, on average, to 1118 microstrain through five weeks, followed by shrinkage, albeit at a slower rate than the MALP and MKP-VO specimens, and continued to maintain net expansion of 812 microstrain at 365 days.

The high values of shrinkage exhibited by the MALP-E, MALP-NE, and MKP-VO specimens, indicate that there may be problems with high crack widths at the edges of repairs with conventional concrete. This is borne out by crack widths measured at the edges of the

repair regions of the field test specimens, which had values on the order of 0.020 in. (20 mils), as shown in Table 3.3. Twenty-mil cracks are considered wide cracks.

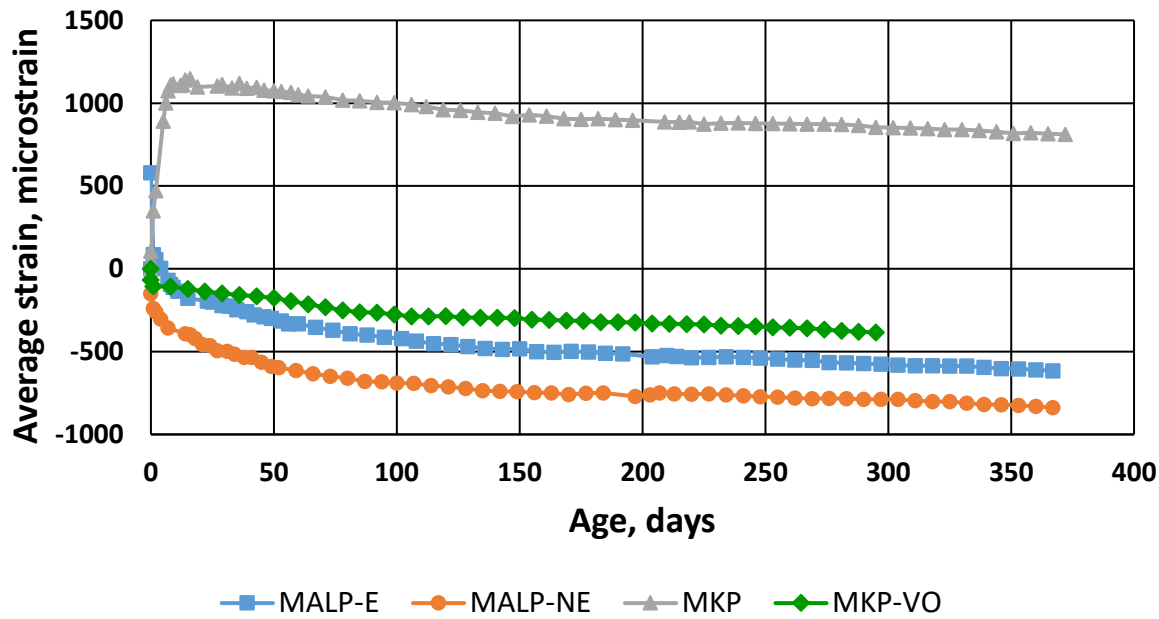


**Figure 3.19-** Average strain in microstrain vs. age after casting for specimens containing MALP, MKP and MKP-VO

**Table 3.3 -** Crack widths at the edges of the repair regions (in.) in field test specimens

Month	MALP-E-B-Conv	MALP-NE-B-Conv	MALP-E-B-Conv-0.6wc	MALP-E-B-Conv-0.6wc-Corr	MALP-E-A-Conv-0.6wc	MALP-E-A-Conv-0.6wc-Corr	MALP-E-A-Conv	MALP-NE-A-Conv
1	0.003	0.003	0.005	0.003	0.005	0.005	0.003	0.003
2	0.005	0.003	0.005	0.005	0.005	0.005	0.003	0.005
3	0.007	0.005	0.007	0.007	0.005	0.007	0.007	0.009
4	0.007	0.005	0.007	0.007	0.007	0.007	-	-
5	0.009	0.007	0.007	0.009	0.007	0.009	-	-
6	0.009	0.007	0.009	0.009	0.007	0.009	-	-
7	0.009	0.009	0.009	0.010	0.009	0.010	-	-
8	0.010	0.009	0.009	0.010	0.009	0.013	-	-
9	0.010	0.010	0.010	0.016	0.009	0.013	-	-
10	0.010	0.010	0.013	0.016	0.010	0.013	-	-
11	0.013	0.013	0.016	0.020	0.010	0.016	-	-
12	0.013	0.013	0.016	0.020	0.013	0.016	-	-
13	0.016	0.016	0.020	-	0.016	-	-	-
14	0.016	0.016	0.020	-	0.016	-	-	-
15	0.020	0.020	0.020	-	0.016	-	-	-
16	0.020	0.020	-	-	-	-	-	-

# CHAPTER 4: ANALYSIS OF TEST RESULTS

This chapter describes the analysis of the test results.

## 4.1 Corrosion resistance

In the beam tests, specimens made with MALP, whether with or without Endure, showed excellent resistance to corrosion. Even though the MALP without Endure (MALP-NE) had slightly more negative corrosion potentials, it never exhibited active corrosion. The same strong performance held true in the beam (B) and cracked beam (CB) specimens when MALP was used in conjunction with regular conventional concrete (MALP/Conv) or even with pre-corroded reinforcement (MALP-E-Corr), where corrosion activity stayed minimal. Overall, the results show MALP provides dependable, long-term protection regardless of the condition of the substrate or reinforcement as long as the material completely encloses the reinforcing steel. By contrast, the MKP specimens began corroding quickly. MKP-VO specimens initially performed much better, showing almost no corrosion during the first 8 weeks. After this initial period of low corrosion activity, however, their rates climbed to match those of regular MKP, followed by a long period of relatively low corrosion activity. This suggests that the MKP-VO concrete gives longer-lasting resistance than MKP.

The control group (conventional concrete) showed moderate corrosion activity in uncracked concrete. The B-Conv specimens exhibited fairly stable corrosion activity up to week 48, but after that, the corrosion rate climbed and stayed elevated until the end of testing. Specimens made with low quality concrete (B-Conv-0.6wc) performed worse, as expected. These fluctuations suggest that more permeable concretes with higher water-to-cement ratios are less able to keep the steel reinforcement passive under chloride exposure, leaving it open to localized attack. The worst performance came from conventional specimens with already corroded reinforcement (B-Conv-0.6wc-Corr). This shows how existing corrosion damage makes steel much more vulnerable, accelerating further deterioration even when conditions are otherwise the same. In contrast, when MALP was combined with low quality concrete, corrosion was almost completely prevented. By week 72, the B-MALP/Conv-0.6wc specimens had macrocell corrosion rates close to zero, and those with pre-corroded reinforcement (B-MALP/Conv-0.6wc-Corr) consistently stayed below 1  $\mu\text{m}/\text{year}$  through 67 weeks.

In cracked beam specimens, those containing MALP maintained excellent corrosion resistance. Specimens combining MALP with conventional concrete (CB-MALP/Conv) exhibited very low macrocell corrosion rates, typically in the range of 1–2  $\mu\text{m}/\text{year}$  and often close to zero. Other MALP formulations, both with and without Endure performed similarly, even with pre-corroded reinforcement. Like the results for the beam specimens, these results highlight MALP's robust protective properties as long as the material completely encloses the reinforcing steel, even when cracking accelerates chloride penetration. As shown in Figure 3.3, the MKP specimens in the cracked beam specimens exhibited active corrosion, similar to their performance in uncracked concrete. MKP-VO specimens followed a comparable trend during the early test period, showing corrosion rates similar to standard MKP between weeks 6 and 23. Afterward, however, their performance improved, with rates falling below 3  $\mu\text{m}/\text{year}$  and remaining at this low level through 96 weeks. This suggests that the MKP-VO formulation will provide some protective capacity over the long term, even when cracking is present.

The results based on macrocell corrosion, however, do not tell the whole story. As shown in Tables 3.1 and 3.2, the cracked beam specimens combined with conventional concrete exhibited very high total corrosion rates, suggesting a significant degree of microcell corrosion. If the increased corrosion resulted from greater access of oxygen and moisture to the bottom bars in the conventional concrete, it is not clear why the greater access of oxygen and moisture did not translate into increased macrocell corrosion, which was not observed. Thus, while the poorer performance of these specimens is clear, the mechanism is not clear.

The cracked conventional concrete specimens (CB-Conv) demonstrated an early increase in corrosion rates, peaking at 17.3  $\mu\text{m}/\text{year}$  at week 15. This was followed by a steady decline to 3.1  $\mu\text{m}/\text{year}$  at week 84, before climbing again to 8.2  $\mu\text{m}/\text{year}$  by week 96. Specimens with low quality concrete and uncorroded reinforcement (CB-Conv-0.6wc) exhibited more severe early corrosion, reaching 22.5  $\mu\text{m}/\text{year}$  at week 25. Corrosion rates then gradually declined to 10  $\mu\text{m}/\text{year}$  by week 55, dropped sharply below 5  $\mu\text{m}/\text{year}$  at week 56, and stabilized near 5  $\mu\text{m}/\text{year}$  through week 84. The most severe corrosion occurred in specimens with low quality concrete and corroded reinforcement (CB-Conv-0.6wc-Corr). These exhibited a sharp rise in rate to 33.24  $\mu\text{m}/\text{year}$  at week 9, followed by fluctuations in rate over time. These unstable and elevated rates demonstrate the combined negative impact of poor-quality concrete and pre-corroded reinforcement. Specimens combining MALP with low quality concrete, with or without corroded reinforcement (CB-MALP/Conv-0.6wc-Corr and CB-MALP/Conv-0.6wc), performed better than conventional concrete specimens. Both maintained corrosion rates below 3  $\mu\text{m}/\text{year}$  from the start of testing up to weeks 67 and 72, respectively. Although their corrosion activity was slightly higher than in uncracked beams, the results confirm that partial substitution with MALP significantly improves durability even in cracked systems.

The field test specimen results (Figures 3.13 and 3.14) show that all specimens at some stage reached potentials more negative than  $-0.35$  V (CSE), indicating active corrosion. Overall, corrosion rates for field test specimens were approximately an order of magnitude lower than those of the laboratory beam tests, which is expected due to the less aggressive exposure and larger specimen size. Monolithic MALP specimens maintained low corrosion rates (less than 0.2  $\mu\text{m}/\text{yr}$ ), even in the presence of cracks, confirming excellent long-term protection. Specimens made of low-quality concrete with a MALP repair patch showed higher and more variable rates, particularly when pre-corroded steel was present, peaking near 5 to 7  $\mu\text{m}/\text{yr}$  around month 12. Conventional concrete specimens, both cracked and uncracked, remained below 2  $\mu\text{m}/\text{yr}$  after sixteen months, while specimens including conventional concrete and a MALP repair patch exhibited greater corrosion depending on patch geometry. When the patch edge aligned directly above the reinforcement (A-type), corrosion rates rose to about 2.5  $\mu\text{m}/\text{yr}$ , indicating easier ingress of moisture and oxygen. These findings demonstrate that substrate quality, patch edge alignment, and presence of cracks at the edge of repairs are critical: cracks and bar aligned interfaces promote localized corrosion, whereas when MALP fully encloses reinforcement, it limits chloride and moisture transport, providing improved corrosion protection to the reinforcing steel.

## 4.2 Freeze-thaw test

For Procedure A (freezing and thawing in water), MALP specimens (with and without Endure) showed excellent durability. All MALP specimens successfully passed more than 1000 cycles without visible cracking or deterioration, demonstrating strong resistance to freeze-thaw damage. In contrast, MKP specimens deteriorated rapidly, with a sharp drop in relative dynamic

modulus. By just 163 cycles, the modulus had fallen to 60% of the initial value, indicating rapid loss of structural integrity. The MKP-VO specimens performed better, maintaining a stable modulus through approximately 500 cycles. However, after this point, they too began to degrade, reaching 63% of the initial modulus at 1019 cycles. MALP-E/Conv (horizontal interface) specimens exhibited an initial gain in modulus during the first 56 cycles, followed by a gradual decline to 76% after 1004 cycles. While these hybrid specimens provided better resistance than MKP, their durability did not match that of pure MALP formulations. In spite of their lower performance level, the MKP-VO and MALP-E/Conv specimens performed well enough to be considered as durable by the usual measures used in this test.

In Procedure B (freezing in air and thawing in water), MKP specimens were highly vulnerable, failing the 95% relative dynamic modulus criterion after less than 30 cycles. By comparison, MALP specimens demonstrated superior resistance, exhibiting an increase in relative dynamic modulus and completing over 1031 freeze-thaw cycles with no signs of deterioration. MKP-VO specimens initially maintained stability, holding their modulus constant for 249 cycles. Afterward, a gradual decline occurred: 90% at 359 cycles, and eventually 60% after 632 cycles. Hybrid MALP-E/Conv horizontal specimens initially gained modulus, but dropped to 56% at 289 cycles. MALP-E/Conv vertical interface specimens failed prematurely at the bond line, highlighting the importance of interface quality in mixed systems.

### **4.3 Scaling test**

In the scaling test, the MALP specimens demonstrated different scaling resistance depending on the presence of Endure, but neither form performed well. The MALP-NE specimens exhibited significantly higher mass loss than the MALP-E specimens, indicating that adding Endure improves scaling resistance. Both MALP-E and MALP-NE, however, exceeded the maximum allowable average cumulative mass loss specified by Quebec Test BNQ NQ 2621-900 (0.10 lb/ft<sup>2</sup>) and the Ministry of Transportation of Ontario (MTO) (0.16 lb/ft<sup>2</sup>) by the end of the test. The results suggest that while MALP concrete performs well under cycles of freezing and thawing, the material may require surface protection to fully meet aggressive salt-scaling environments. In contrast, MKP and MKP-VO exhibited excellent scaling resistance. Both maintained near-zero mass loss after 56 cycles, well within the limits of BNQ and MTO standards. The results indicate that MKP-based systems are highly resistant to surface scaling under the test conditions.

### **4.4 Shrinkage test**

In the free shrinkage test, MALP specimens exhibited measurable shrinkage, with performance depending on the presence of Endure. MALP without Endure (MALP-NE) showed the greatest shrinkage values, indicating higher susceptibility to drying shrinkage stresses. In contrast, MALP with Endure (MALP-E) demonstrated reduced shrinkage, confirming the beneficial role of the Endure additive in mitigating shrinkage-induced dimensional changes. Unlike MALP, MKP specimens initially underwent expansion during the first five weeks. This was followed by a transition into shrinkage, although at a slower rate than MALP. Over the entire test duration, MKP specimens continued to demonstrate net expansion, suggesting a fundamentally different volumetric response compared to MALP concrete. MKP-VO specimens were not part of the original study but were later included to assess shrinkage behavior. After 295 days, MKP-VO specimens displayed lower shrinkage than MALP-E specimens, but they did not exhibit the early expansion observed in standard MKP specimens.

The free shrinkage test results are supplemented by the crack-width measurements obtained from the field tests corrosion test specimens. Those specimens indicate that cracks at the interface of repairs can reach 20 mils (0.020 in.) in 11 to 15 months. Cracks this wide provide a ready path for water, oxygen, and deicing chemicals, which can greatly reduce the protection provided by MALP repairs. This behavior is the likely reason for the relative poor corrosion performance of the field test specimens with the simulated repair regions.

# CHAPTER 5: SUMMARY AND CONCLUSIONS

## 5.1 Summary

The performance of a proprietary magnesium-alumino-liquid-phosphate (MALP) concrete, marketed under the trade name Phoscrete, with and without Endure, an organic admixture designed to improve the resistance of MALP to freeze-thaw damage and salt scaling, was evaluated and compared with magnesium-potassium-phosphate (MKP) concrete and an MKP formulation for vertical and overhead placement (MKP-VO). MALP concrete is known for its rapid setting and strength gain, and the ability to provide corrosion protection, while MKP provides longer working time and comparable early strength development. The inclusion of the organic admixture Endure was also examined to improve resistance against freeze-thaw cycles and scaling.

To assess these materials, the experimental program included more than 120 laboratory corrosion specimens, 16 field test specimens, 39 freeze-thaw specimens, 24 scaling specimens, and 39 shrinkage specimens. The corrosion behavior was evaluated using both bench-scale tests (beam and cracked-beam specimens) and field test specimens, allowing assessment of performance in uncracked and cracked conditions, with both uncorroded and corroded reinforcing steel. Measurements include both macrocell and total corrosion. Freeze-thaw durability was investigated under ASTM C666 Procedures A and B, while surface scaling resistance was evaluated in accordance with BNQ NQ 2621-900 and MTO standards. In addition, free shrinkage tests were conducted over a one-year period to quantify dimensional stability and crack width development was monitored at the repair interfaces in the field test corrosion test specimens.

## 5.2 Conclusions

The following conclusions are based on the experimental results and analyses presented in this report.

1. MALP specimens, with and without Endure, in which MALP completely enclosed the reinforcing steel (beam, cracked beam, and field test specimens) exhibited excellent corrosion performance throughout the test period.
2. The half MALP/conventional concrete beam and cracked beam specimens also showed very low macrocell corrosion rates. The MALP/conventional concrete cracked beam specimens exhibited high total corrosion rates.
3. The field test specimens with MALP repair regions provided poorer corrosion performance than similar specimens (with and without simulated cracks) cast with good quality conventional concrete, suggesting that the presence of cracks at the interface between the repair region and the conventional concrete permits water, oxygen, and deicing chemicals to reach the reinforcing steel.
3. The MKP beam and cracked beam specimens displayed active corrosion in both beam and cracked beam specimens.

4. The MKP-VO beam and cracked beam specimens showed improved performance compared to MKP: corrosion rates were similar to MKP early on but dropped and remained approximately stable through 96 weeks.

5. The MALP specimens, especially those containing Endure, showed only slight differences between macrocell and total corrosion, indicating stable and uniform protection. In contrast, MKP and conventional concretes exhibited much greater differences, suggesting more localized and aggressive corrosion behavior.

6. In the freeze–thaw test, the MALP specimens with or without Endure showed excellent durability, while MKP failed quickly and MKP-VO performed moderately but degraded over time. Specimens MALP-E/Conv (horizontal interface) showed moderate durability, performing well under procedure A but exhibiting reduced resistance under procedure B.

7. In the scaling test, MALP with Endure performed better than MALP without Endure but both exceeded BNQ and MTO limits, indicating a need for a protective layer to improve surface protection. In contrast, MKP and MKP-VO showed excellent scaling resistance, maintaining near to zero mass loss.

8. In the shrinkage test, MALP specimens showed continuous shrinkage, with Endure reducing the effect, while MKP exhibited initial expansion followed by shrinkage at a slower rate. MKP-VO showed lower shrinkage than MALP but did not expand like MKP.

### **5.3 Recommendations**

1. Evaluate scaling resistance MALP with modified Endure dosages or other protective coatings.
2. Evaluate use of MALP to provide corrosion protection to reinforcing steel in conjunction with MKP and MKP-VO in repairs of conventional concrete.
3. Investigate the performance of MKP-VO under field conditions.
4. Perform freeze–thaw resistance studies for using MALP and MKP-VO in horizontal and vertical interfaces.

## CHAPTER 6: REFERENCES

ASTM C157/C157M-17, 2017. Standard Test Method for Length Change of Hardened Hydraulic-Cement Mortar and Concrete, ASTM International, West Conshocken, PA, 8 pp.

ASTM C215-19, 2019. Standard Test Method for Fundamental Transverse, Longitudinal, and Torsional Resonant Frequencies of Concrete Specimens, ASTM International, West Conshocken, PA, 7 pp.

ASTM C666/C666M-15, 2015. Standard Test Method for Resistance of Concrete to Rapid Freezing and Thawing, ASTM International, West Conshocken, PA, 7 pp.

ASTM C672/C672M-12, 2012. Standard Test Method for Scaling Resistance of Concrete Surfaces Exposed to Deicing Chemicals, ASTM International, West Conshocken, PA, 3 pp. Withdrawn 2021.

ASTM C876-22b, Standard Test Method for Corrosion Potentials of Uncoated Reinforcing Steel in Concrete, In Annual Book of ASTM Standards, ASTM International, 2022, West Conshohocken, USA

ASTM G109-21, 2021. Standard Test Methods for Determining Effects of Chemical Admixtures on Corrosion of Embedded Steel Reinforcement in Concrete Exposed to Chloride Environments, ASTM International, West Conshocken, PA, 6 pp.

Floyd, R. W., Volz, J. S., Looney, Trevor, Mesigh, M., Ahmadi, M., Roswurm, S., Huynh, P., and Manwarren, M., 2021. "Evaluation of Ultra-High Performance Concrete, Fiber Reinforced Self-Consolidating Concrete, and MALP Concrete for Prestressed Girder Repair," *Final Report*, FHWA-OK-21-03, ODOT SPR Item Number 2284, 313 pp.

Lindquist, W. D., Darwin, D., Browning, J., and Miller, G. G., 2006. "Effect of Cracking on Chloride Content in Concrete Bridge Decks," *ACI Materials Journal*, Vol. 103, No. 6, Nov.-Dec. pp. 467-473.

Phoscrete Corporation. 2021. *Stop Rust and Mitigate the Halo Effect*, Technical Report, 1 pp.

Qin, J., Dai, F., Ma, H., Dai, X., Li, Z., Jia, X., and Qian, J. 2022. "Development and Characterization of Magnesium Phosphate Cement Based Ultra-High Performance Concrete," *Composites Part B*, 234, 109694.

Ramsey, M. A., Scott, D. A., Weiss Jr., C. A., and Tingle, J. S. 2020. "Development of Magnesium Phosphate Cement (MPC) Concrete Mixture Proportioning for Airfield Pavements," *Polymers, ERDC /GSL TR 20 4*, U.S. Army Engineer Research and Development Center, 118 pp.

Zhang, L., Jiang Z., Zhang W., Peng, S., and Chen, P. 2020. "Flexural Properties and Microstructure Mechanisms of Renewable Coir-Fiber-Reinforced Magnesium Phosphate Cement-Based Composite Considering Curing Ages," *Polymers*, 12, 2556.